166

0-315-12480-6

National Library of Canada
Bibliothèque nationale du Canada

Canadian Theses Division
Division des thèses canadiennes

Ottawa, Canada
K1A 0N4

60391

PERMISSION TO MICROFILM — AUTORISATION DE MICROFILMER

• Please print or type — Écrire en lettres moulées ou dactylographier

Full Name of Author — Nom complet de l'auteur

PRADEEP KUMAR AGGARWAL

Date of Birth — Date de naissance	Country of Birth — Lieu de naissance
Sept. 11, 1956	INDIA

Permanent Address — Résidence fixe

E-148, Nanakpur
New Delhi -110 021, INDIA

Title of Thesis — Titre de la thèse

Geochemistry of the Chu Chua Massive Sulfide Deposit, British Columbia

University — Université

University of Alberta

Degree for which thesis was presented — Grade pour lequel cette thèse fut présentée

M.Sc.

Year this degree conferred — Année d'obtention de ce grade	Name of Supervisor — Nom du directeur de thèse
1982	Dr. Bruce E. Nesbitt

Permission is hereby granted to the NATIONAL LIBRARY OF CANADA to microfilm this thesis and to lend or sell copies of the film.

The author reserves other publication rights, and neither the thesis nor extensive extracts from it may be printed or otherwise reproduced without the author's written permission.

L'autorisation est, par la présente, accordée à la BIBLIOTHÈQUE NATIONALE DU CANADA de microfilmer cette thèse et de prêter ou de vendre des exemplaires du film.

L'auteur se réserve les autres droits de publication; ni la thèse ni de longs extraits de celle-ci ne doivent être imprimés ou autrement reproduits sans l'autorisation écrite de l'auteur.

Date	Signature
Oct. 15/82	P. K. Aggarwal

NL-91 (4/77)

CANADIAN THESES ON MICROFICHE

I.S.B.N.

THESES CANADIENNES SUR MICROFICHE

National Library of Canada
Collections Development Branch

Canadian Theses on
Microfiche Service

Ottawa, Canada
K1A 0N4

Bibliothèque nationale du Canada
Direction du développement des collections

Service des thèses canadiennes
sur microfiche

NOTICE

The quality of this microfiche is heavily dependent upon the quality of the original thesis submitted for microfilming. Every effort has been made to ensure the highest quality of reproduction possible.

If pages are missing, contact the university which granted the degree.

Some pages may have indistinct print especially if the original pages were typed with a poor typewriter ribbon or if the university sent us a poor photocopy.

Previously copyrighted materials (journal articles, published tests, etc.) are not filmed.

Reproduction in full or in part of this film is governed by the Canadian Copyright Act, R.S.C. 1970, c. C-30. Please read the authorization forms which accompany this thesis.

THIS DISSERTATION
HAS BEEN MICROFILMED
EXACTLY AS RECEIVED

AVIS

La qualité de cette microfiche dépend grandement de la qualité de la thèse soumise au microfilmage. Nous avons tout fait pour assurer une qualité supérieure de reproduction.

S'il manque des pages, veuillez communiquer avec l'université qui a conféré le grade.

La qualité d'impression de certaines pages peut laisser à désirer, surtout si les pages originales ont été dactylographiées à l'aide d'un ruban usé ou si l'université nous a fait parvenir une photocopie de mauvaise qualité.

Les documents qui font déjà l'objet d'un droit d'auteur (articles de revue, examens publiés, etc.) ne sont pas microfilmés.

La reproduction, même partielle, de ce microfilm est soumise à la Loi canadienne sur le droit d'auteur, SRC 1970, c. C-30. Veuillez prendre connaissance des formules d'autorisation qui accompagnent cette thèse.

LA THÈSE A ÉTÉ
MICROFILMÉE TELLE QUE
NOUS L'AVONS REÇUE

NL-339 (r. 82/08)

Canada

THE UNIVERSITY OF ALBERTA

Geochemistry Of The Chu Chua Massive Sulfide Deposit, British Columbia

by

© Pradeep Kumar Aggarwal

A THESIS

SUBMITTED TO THE FACULTY OF GRADUATE STUDIES AND RESEARCH

IN PARTIAL FULFILMENT OF THE REQUIREMENTS FOR THE DEGREE

OF Master of Science

The Department of Geology

EDMONTON, ALBERTA

Fall, 1982

Microfilm

THE UNIVERSITY OF ALBERTA

RELEASE FORM

NAME OF AUTHOR Pradeep Kumar Aggarwal

TITLE OF THESIS Geochemistry Of The Chu Chua Massive Sulfide Deposit, British Columbia

DEGREE FOR WHICH THESIS WAS PRESENTED Master of Science

YEAR THIS DEGREE GRANTED Fall, 1982

Permission is hereby granted to THE UNIVERSITY OF ALBERTA LIBRARY to reproduce single copies of this thesis and to lend or sell such copies for private, scholarly or scientific research purposes only.

The author reserves other publication rights, and neither the thesis nor extensive extracts from it may be printed or otherwise reproduced without the author's written permission.

(SIGNED) P.K. Aggarwal

PERMANENT ADDRESS:

E-148, Nanakpur

NEW DELHI 110021

INDIA

DATED October 15, 1982

THE UNIVERSITY OF ALBERTA

FACULTY OF GRADUATE STUDIES AND RESEARCH

The undersigned certify that they have read, and recommend to the Faculty of Graduate Studies and Research, for acceptance, a thesis entitled Geochemistry Of The Chu Chua Massive Sulfide Deposit, British Columbia submitted by Pradeep Kumar Aggarwal in partial fulfilment of the requirements for the degree of Master of Science.

Bruce E. Warbritt

Supervisor

Date October 1, 1982.

Dedication

To my parents

Abstract

The Chu Chua massive sulfide deposit, located in southcentral British Columbia, occurs in the mafic volcanic rocks of the upper Paleozoic Fennell Formation. The Fennell Formation consists of basalts and associated marine sediments metamorphosed at low-greenschist facies conditions. Although the microphenocrysts of plagioclase and Fe - Ti oxides are almost completely altered, those of augite and amphibole have survived this metamorphism. Relict augite microphenocrysts are enriched in Al and Ti and are similar in composition to those of alkalic and subalkalic basalts from Hawaii and the deep-sea. Relict amphiboles are also enriched in Ti (4.5% to 5.9% TiO_2) and are classified as kaersutites. Occurrence of kaersutite and the chemistry of relict augites indicate that the Fennell Formation basalts were originally alkalic and transitional in composition.

However, the whole-rock chemical composition of these basalts are apparently similar to abyssal tholeiites. Even on the conventional Ti - Zr and Ti - Zr/P_2O_5 immobile element discrimination diagrams, both the kaersutite-bearing and kaersutite-free rocks plot in the tholeiitic basalt field. Based on these observations, it is suggested that the immobile element discrimination diagrams may not provide unambiguous evidence for identifying the magmatic composition of altered volcanic rocks.

The lead isotopic compositions of the Fennell Formation basalts are more radiogenic than those of the MORBs This, together with their petrographical dissimilarities with abyssal tholeiites and alkalic character, suggests that the rocks of the Fennell Formation were formed in a tectonic setting similar to the present-day ocean islands or seamounts.

The deposit consists of two major, lensoid massive sulfide bodies composed mainly of pyrite and chalcopyrite. These sulfide bodies are underlain by massive silicic and talcose rocks which have very low Al, Ti, Zr and P contents. This suggests that the silicic and the talcose rocks are chemical precipitates and not produced by the alteration of the host basalts. Stabilities of talc, pyrrhotite, pyrite, chalcopyrite and magnetite as a function of fO_2 - pH are consistent with a primary origin for these rocks. Also, it is indicated that talc may have been deposited in areas of relatively higher temperature (300°C and above) and lower oxygen fugacity compared with the sulfide and silica minerals. These areas of talc deposition are suggested to represent the vents of the

ore-forming solutions. The lead isotopic compositions of pyrite and chalcopyrite are similar to those of the host basalts suggesting that these basalts or the basement rocks were the most likely source of metals in the hydrothermal solutions. It is proposed that chemically precipitated silicic and talc rocks may be used as exploration guides for massive sulfides associated with alkalic basalts in an ocean island tectonic setting.

Acknowledgements

I record with gratitude my thanks to Bruce Nesbitt who, as my supervisor, provided invaluable guidance from the begining to the completion of this project. I also thank Roger Morton for suggesting and initiating this project. Thanks are due to the owners of the Chu Chua property, the Craigmont Mines Ltd., Vestor Exploration Ltd., and the Seaforth Mines Ltd., for allowing acess to their property and to Nels Vollo of Craigmont for help during the field work.

I am indebted to Toshi Fujii for the critical discussions on the petrological aspects of the project. Dr. H. Baadsgaard is thanked for generous help and guidance in the lead isotope analyses. I thank Steve Launspach for sharing with me his expertise in the operation of the electron-probe and data processing.

Many other faculty and colleagues extended their cooperation for which I am thankful to them. Fred Longstaffe and Bob St. Louis are specially thanked for being a source of moral encouragement.

Financial support for this project was provided by the Boreal Institute for Northern Studies and a teaching assistantship to the author from the Department of Geology, and is gratefully acknowledged.

Table of Contents

Chapter		Page
I.	Introduction	1
II.	Magmatic Composition and Tectonic Setting of Volcanic Rocks of The Fennell Formation, British Columbia	2
	A. Introduction	2
	B. Geological Setting	2
	C. Petrography	4
	D. Analytical Procedures	8
	E. Analytical results	9
	F. Discussion	13
	Initial composition of the volcanic rocks	13
	Tectonic Setting	23
III.	Conclusions	27
IV.	Geochemistry of the Chu Chua Massive Sulfide Deposit, British Columbia	28
	A. Introduction	28
	B. Local Geology	28
	Sulfide bodies	32
	Wall rocks	35
	Origin of the footwall rocks	37
	C. Environment of Deposition	38
	Solution Parameters	38
	Discussion	39
	D. Genetic Model	44
	Applications to exploration for Cu–Fe massive sulfide deposits	48
V.	Conclusions	51
VI.	References	52
VII.	Appendix I: Sample Locations And Mineral Assemblages	57
VIII.	Appendix II: Chemical Analyses	63
IX.	Appendix III: Construction of fO_2 – pH Diagrams	67

List Of Tables

Table 1: Representative whole-rock analyses of basaltic rocks of the Fennell Formation 10

Table 2: Representative analyses of augite microphenocrysts in basalts from Chu Chua 11

Table 3: Representative analyses of amphibole microphenocrysts in basalts from Chu Chua 12

Table 4: Lead isotopic composition of Fennell Formation basalts 25

Table 5: Whole-rock analyses of the silicic and the talc units from the Chu Chua deposit 36

Table 6: Lead isotopic composition of pyrite and chalcopyrite from the Chu Chua deposit 45

List Of Figures

Figure 1: Regional geological map of southcentral British Columbia 3

Figure 2: Quadrilateral plot of augite compositions 15

Figure 3: Ca+Na vs Ti(cation proportion) content of augites 17

Figure 4: Fe^{2+}/Fe^{2+}+Mg vs Ti content of augites 19

Figure 5: Ti – Zr/P_2O_5 diagram for discriminatomn between alkalic and tholeiitic basalts 20

Figure 6: Ti – Zr discrimination diagram 21

Figure 7: P_2O_5 – Zr content of basalts from Chu Chua 22

Figure 8: Lead isotopic composition of Fennell Formation basalts from Chu Chua 26

Figure 9: Local geological map of the Chu Chua area 29

Figure 10: Horizontal sections through the Chu Chua ore bodies 30

Figure 11: Vertical sections through the Chu Chua ore bodies 31

Figure 12: fO_2 – pH diagram at 300°C 40

Figure 13: fO_2 – pH diagram at 250°C 41

Figure 14: Pb isotopic composition of pyrite and chalcopyrite from Chu Chua 46

Figure 15:Schematic sketch for the genesis of the Chu Chua ore deposit 49

List Of Plates

Plate 1: Glomeroporphyritic microphenocrysts of plagioclase 6

Plate 2: Subhedral grains and laths of augite microphenocrysts 6

Plate 3: Red-brown, prismatic amphibole microphenocrystsin basalts at Chu Chua 7

Plate 4: Altered microphenocrysts of Fe - Ti oxides 7

Plate 5: Fine intergrowths of Pyrite - Chalcopyrite - Sphalerite displaying colloform texture 33

Plate 6: Subhedral grains of pyrite showing triple-point junction texture 33

Plate 7: Annealing twins in chalcopyrite 34

Plate 8: Fine-grained anhedral quartz and phengite in silicic unit 34

I. Introduction

Numerous occurrences of mineralisation are known in the upper Paleozoic volcanic–sedimentary sequences of the Eagle–Bay and Fennell Formations in southcentral British Columbia (Preto, 1979). Most of these Cu, Pb and Cu – Pb – Zn occurrences are in the felsic volcanic rocks of the Eagle–Bay Formation (Vollo, 1981). The Chu Chua deposit is the first reported massive sulfide deposit in the rocks of the Fennell Formation which are mainly basaltic in composition (Campbell and Tipper, 1971; Hall–Bayer, 1976; Preto, 1979; Preto and Schiarriza, 1982). This deposit was discovered in 1978 following stream–sediment geochemical surveys and has been explored through geophysical surveys and drilling. It consists of Cu – Fe sulfide bodies with associated massive talc, talc–magnetite, and silicic rocks. In order to develop exploration criteria for massive sulfides in the region, it is imperative to understand the petrogenesis of the host rocks and the genesis of the deposit.

This thesis reports the geological and geochemical investigations of the rocks and ores from the Chu Chua area undertaken to achieve the above objectives. The results are presented in two parts. In the first part, the initial magmatic composition and paleo–tectonic setting of the rocks of the Fennell Formation are established using a variety of geochemical criteria, particularly, the compositions of the relict minerals.

The second part deals with the geological and genetic aspects of the ore deposit. The geological features of the sulfide bodies and the footwall rocks reveal characteristic associations of the sulfide, silicate and oxide minerals. These associations impose constraints on the solution parameters for the thermodynamic calculations used in reconstructing the physical and chemical environment of deposition of the ores and the footwall rocks.

A total of 6000 meters of core from forty–two drill holes was logged and sampled on site (appendix I). Thin– and polished–sections of 150 samples from various rock units and ore were examined for petrographical and mineralogical analyses. The approach was to characterise the different lithologies in terms of their mineralogical and chemical composition and identify any variations with distance from the ore bodies. These data were then used in combination with the thermodynamic considerations on the relative stabilities of minerals to understand the genesis of the host rocks and the ore.

II. Magmatic Composition and Tectonic Setting of Volcanic Rocks of The Fennell Formation, British Columbia

A. Introduction

Considerable effort has been made in recent years to identify the magmatic composition and tectonic environment of altered, volcanic rocks based on geochemical criteria. To see through the effects of alteration and metamorphism, several discrimination diagrams using the relatively immobile elements such as Ti, Y, P, Zr and Nb (Cann, 1970; Humphris and Thompson, 1978b) have been published (Pearce and Cann, 1973; Floyd and Winchester, 1975). These diagrams are commonly used to identify the magmatic composition and tectonic setting of altered rocks of paleo-volcanic series (Bevins, 1981; Grenne and Roberts 1980). The basaltic rocks of the Fennell Formation have been previously classified as abyssal tholeiites based on major element chemistry and immobile elements discrimination diagrams (Hall-Bayer, 1976). In contrast, the petrographic features and relict mineral chemistry of these rocks bear distinct dissimilarities with the present-day abyssal tholeiites.

The object of this study is to identify the magmatic composition and paleo-tectonic setting of the altered, volcanic rocks of the Fennell Formation on the basis of petrography, relict mineral chemistry, and lead isotopic compositions. It will be shown that classification of altered volcanic rocks only on the basis of the immobile elements discrimination diagrams may be ambiguous and, therefore, must be accompanied by detailed petrographical and mineralogical studies which provide more reliable criteria.

B. Geological Setting

The Fennell Formation, correlated with the Antler Formation of the Slide Mountain Group in southcentral British Columbia, forms a part of the upper Paleozoic 'Eastern Tectonostratigraphic Assemblage' of the Canadian Cordillera (Monger, 1977). Regional geological relationships of the Fennell Formation are shown in Figure 1. To the west, it has a faulted contact with the volcanic, Nicola and Cache Creek Groups and the Guichon batholith; and to the east, it is flanked by the volcanic and sedimentary rocks of the Eagle

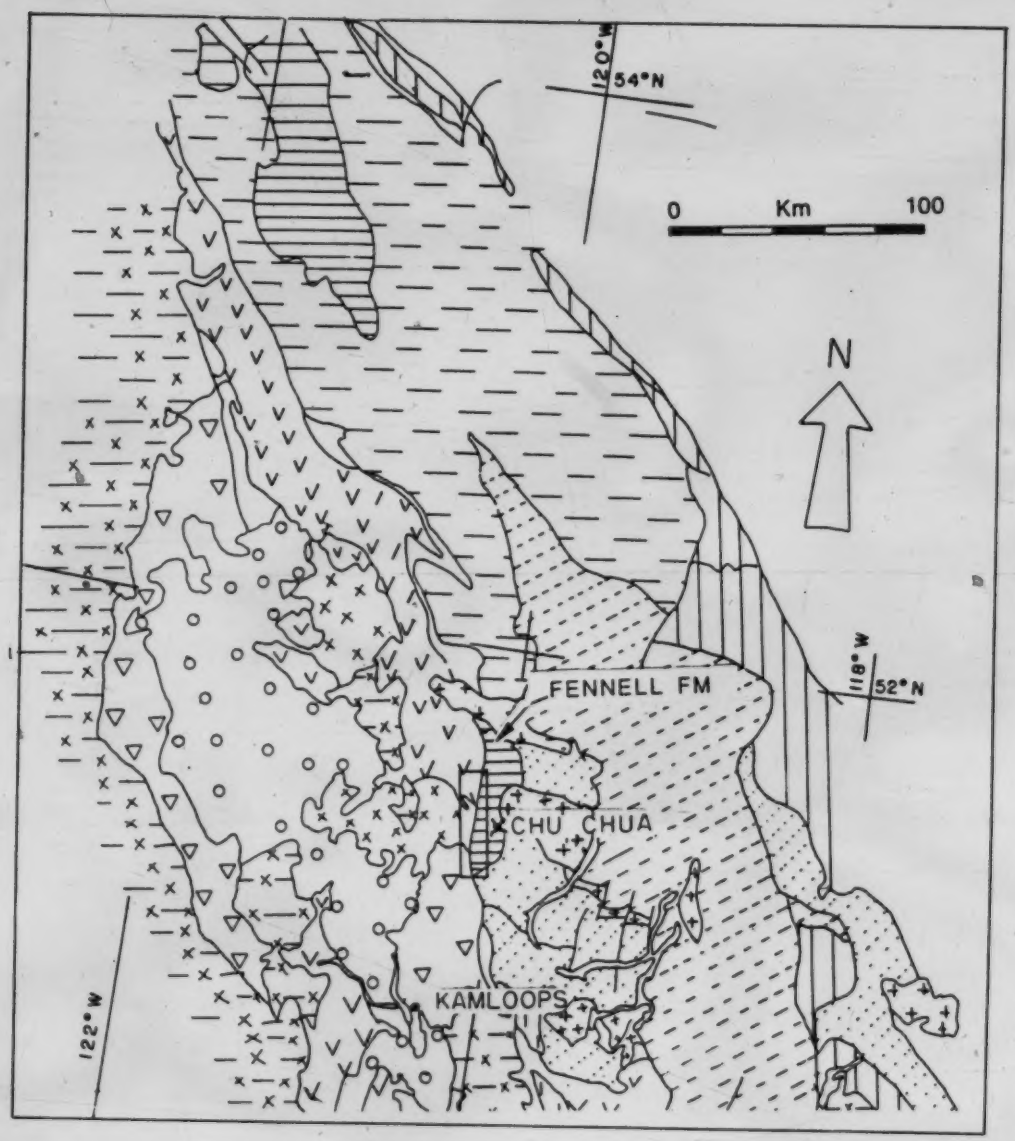

Figure 1. Regional Geological Map of Southcentral British Columbia and Location of Present and Previous Studies

Bay Formation (Campbell and Tipper, 1971; Preto, 1979). In their northern portions, the Fennell and Eagle Bay Formations are intruded by two large, granitic bodies of the Cretaceous Baldy Batholith. The stratigraphic and age relationships between the Fennell and Eagle Bay Formations are not well established. Campbell and Tipper (1971) thought that the Fennell Formation overlies the Eagle Bay Formation with an unconformable or faulted contact. Campbell and Okulitch (1976) proposed that the contact was a low angle fault while Preto (1979) suggested that the Eagle Bay conformably overlies the Fennell Formation. On the basis of isotopic dating of zircons from a quartz-porphyry, unit and with evidence from conodonts in the sedimentary units, Preto and Schiarriza (1982) recently suggested that the Eagle Bay Formation of late Devonian to upper Mississipian age is overlain by the upper Mississipian to late Permian Fennell Formation.

The Eagle Bay and Fennell Formations have been structurally deformed and three phases of mesoscopic folding have been recognised (Campbell and Okulitch, 1973; Preto, 1979). These authors suggest that the earliest phase consists of generally tight, isoclinal mesoscopic folds with recumbent axial planes parallel to the schistosity. The axes of these folds have gentle plunges and trend anywhere from northeasterly to northwesterly. The second stage folds, ranging from a few centimeters to several scores of meters, have upright axial planes with the fold axes plunging gently to the north or northwest (Preto, 1979). A later, and probably minor, stage of folding has produced broad, northerly trending open folds.

The Fennell Formation consists of volcanic greenstones with minor interbedded chert and argillite, concordant bodies of quartz-porphyry and small carbonate lenses. It can be divided into two crudely defined stratigraphic divisions: the lower, eastern division consisting of both intrusive and extrusive phases and interbedded sedimentary units; and the upper, western division consisting mainly of massive- and pillowed-basalts with minor interbedded chert (Campbell and Tipper, 1971; Preto and Schiarriza, 1982).

C. Petrography

The petrographic features of some parts of the Fennell Formation (Fig. 1) have previously been described by Campbell and Tipper (1971) and by Hall-Bayer (1976). According to these authors, the volcanic rocks of the Fennell Formation are fine-grained,

phyric or aphyric basalts. They noted that despite the low-grade metamorphism of these rocks, primary igneous textures and phenocrysts of mafic minerals are still preserved.

Similar features were observed in the samples of this study. Most commonly, glomeroporphyritic or discrete microphenocrysts are set in a matrix of sub-ophitic or intersertal texture (Plate 1). Augite and plagioclase are the major minerals occurring both as microphenocrysts and in the groundmass. Olivine, or its pseudomorph, is noticeably scarce or absent. Pale-brown to colorless augite microphenocrysts (prismatic, subhedral, moderate birefringence, extinction angle ¬40°) occur as subhedral laths or grains(Plate 2). Microphenocrysts of Fe-Ti oxides are also commonly present. At times, a prismatic, red-brown amphibole (pleochroic scheme: X=pale brown, Y=Z=dark reddish brown) occurs as a primary phase or replaces augite (Plate 3). Previous workers (Campbell and Tipper, 1971; Hall-Bayer, 1976) also recorded the presence of an amphibole and identified it as hornblende. However, the occurrence of hornblende is inconsistent with their interpretation of low-grade metamorphism of these rocks. The most common species of amphibole in mafic rocks subjected to low-grade metamorphism is actinolite (Winkler, 1979). In addition, this is inconsistent with the tholeiitic nature of these rocks as suggested by these authors for amphibole is not a stable liquidus phase in a tholeiitic magma (Carmichael *et al.*, 1974) Chemical analyses of amphiboles from rocks of this study, presented in a later section, indicate that they are kaersutites. It is possible that the phase identified as hornblende in other parts of the Fennell Formation might also be kaersutite.

Various types of alteration, of both phenocryst and groundmass minerals, are present in the basalts. Augite and kaersutite phenocrysts are generally altered to actinolite and sphene along cleavages and fractures. Phenocrysts of plagioclase are almost completely albitised and those of titanomagnetite-ilmenite are altered to rutile, hematite and sphene-leucoxene (Plate 4). The groundmass minerals are totally replaced by actinolite, chlorite, albite, clinozoisite, sphene-leucoxene, quartz, and calcite. The secondary mineral assemblage suggests that these basalts have been subjected to metamorphism of low greenschist facies (Winkler, 1979).

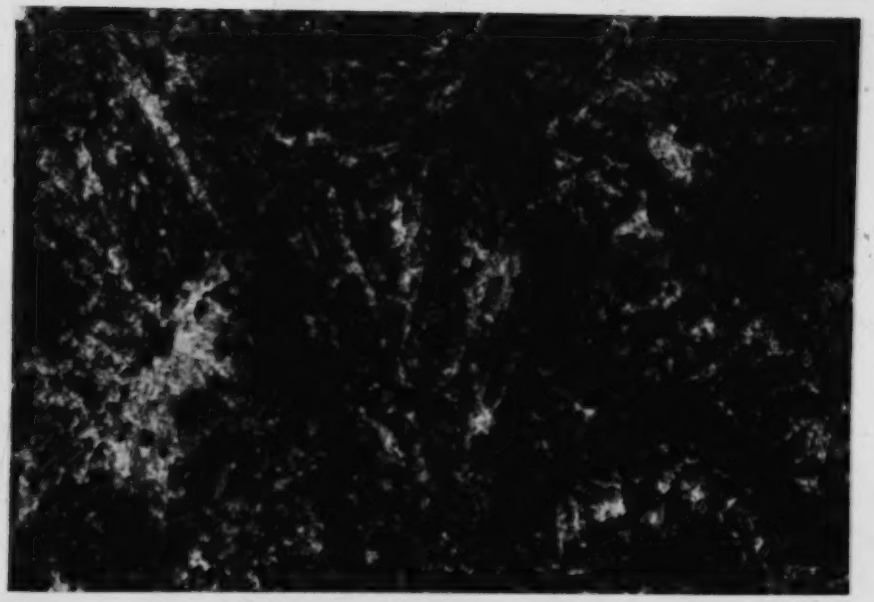

Plate 1. Glomeroporphyritic Microphenocrysts of Plagioclase in Fennell Formation Basalts. (in ppl).

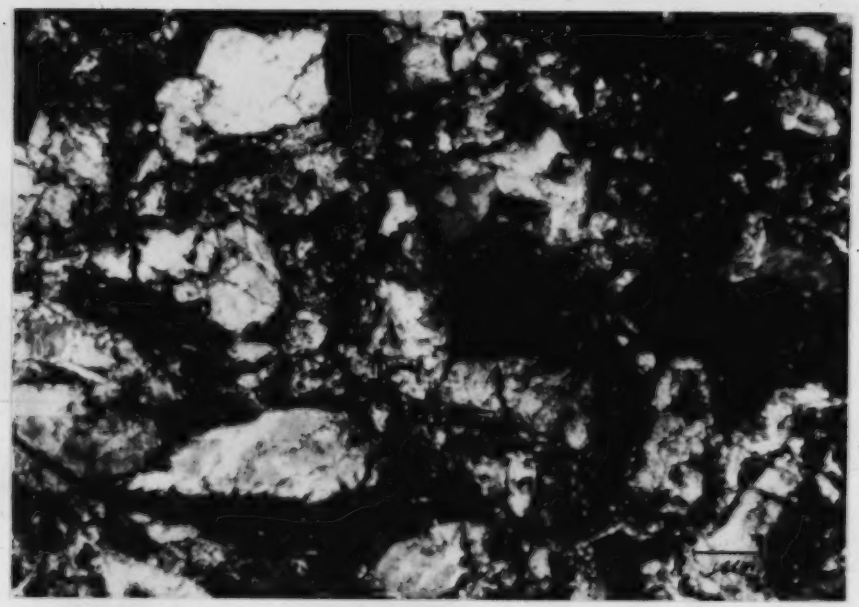

Plate 2. Subhedral Grains and Laths of Augite in the Basalts at Chu Chua. (in X-polars)

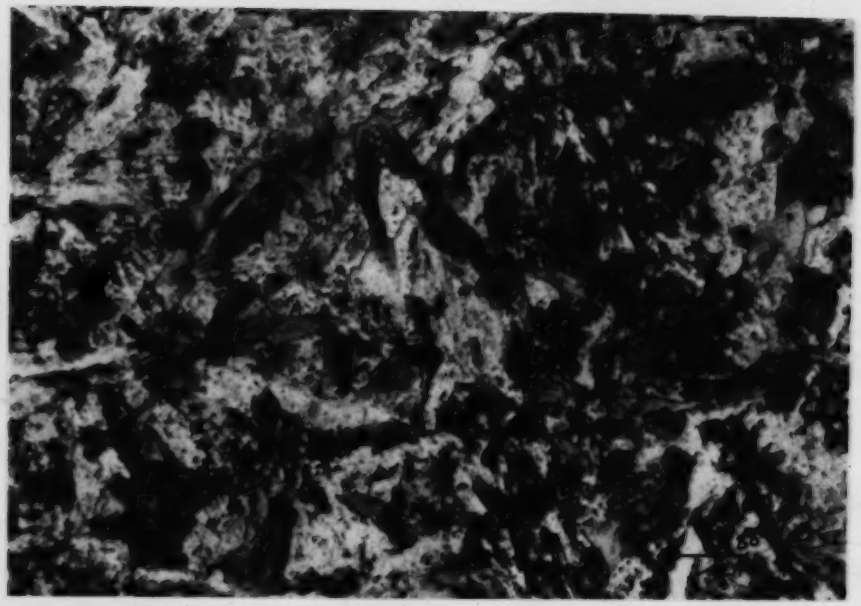

Plate 3. Red-Brown, Prismatic Amphibole in Basalts at Chu Chua. (in ppl)

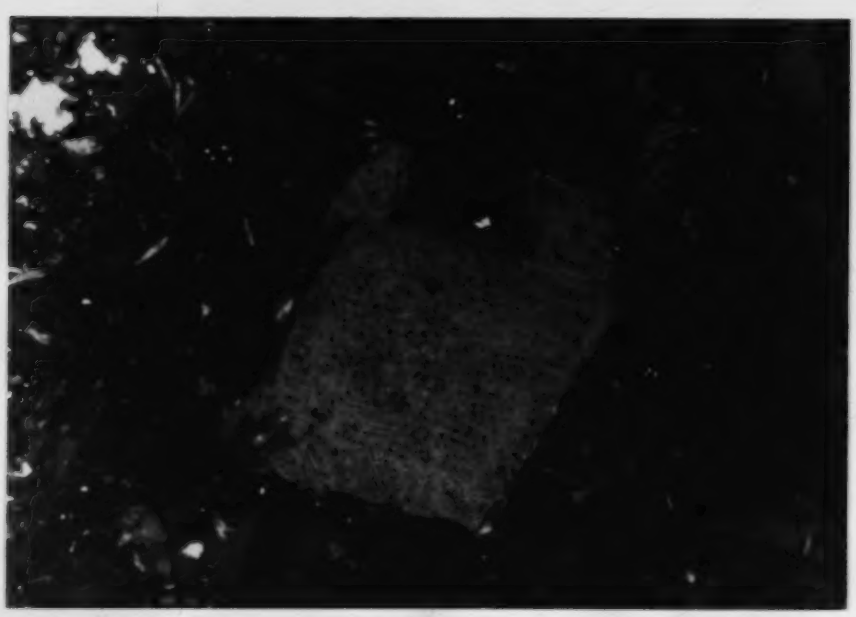

Plate 4. Altered Microphenocrysts of Fe - Ti Oxides in Fennell Formation Basalts. (in reflected light

D. Analytical Procedures

Whole-rock analyses: The whole-rock analyses were performed by the XRF technique at the McMaster University. Two grams of whole-rock sample, crushed and then ground in a tungsten carbide swing mill, were fused with lithium tetraborate. The fused sample were recrushed and pressed into pellets. These pellets were analysed for major, minor and trace elements using an XRF machine. The X-ray intensities were corrected for matrix and background effects. The error of measurement at one sigma level is ± 0.05% for major elements and nearly ± 5% for minor elements which are present in amounts less than 1%. The detection limit for the trace elements is 3 ppm and the error of measurement is less than ± 5%. A detailed discussion of the procedure, accuracy and precision is given in Longstaffe (1978, appendix IV).

Mineral analyses: Analyses of amphiboles and pyroxenes were done at the University of Alberta by the energy-dispersive technique using an ARL - EMX electron microprobe fitted with an ORTEC energy-dispersive spectrometer. Accelerating voltage of 15KV and and a filament current of 0.28 micro-amperes were used. Counting time for both the standards and the samples was 400 seconds. The standards used were: kaersutite for Al, Na, K and Ti; diopside for Mg, Ca and Si and hematite for Fe. The data were processed by the program EDATA2 (Smith and Gold, 1979). The detection limit of the analyses is 0.1 wt%. The statistical error at 99% confidence level is nearly ±1% of the amount present for the major elements and may be as high as ±10% for minor elements.

Lead isotopes: Two grams of powdered whole-rock sample were dissolved in aqua-regia and hydrofluoric acid. Lead was seperated by anion-exchange and loaded on a rhenium filament by the phosphoric acid - silica gel technique. Isotopes were analysed on a solid-source, Micromass - 30, mass spectometer at The University of Alberta. The error of measurement at one sigma level (standard error of the weighted mean) is ±0.05%. The isotopic compositions were corrected for instrumental fractionation effects and normalised with respect to the NBS 981 - common lead standard. The details of this procedure are given in Krstic (1981).

E. Analytical results

Whole-rock: The whole-rock compositions of representative samples [1] of the Fennell Formation basalts are given in Table 1. Only those samples which displayed minimum alteration in thin section were selected for analysis. All compositions are recalculated to 100% on a volatile-free basis. The water content generally ranges between 2 to 4 wt%. These whole-rock compositions are characterised by very low potassium (0.4-0.3% K_2O), high titanium (1.6-2% TiO_2) and high phosphorous (0.20-0.23% P_2O_5) contents. For comparison, composition of rocks from other parts of the Fennell Formation (Hall-Bayer, 1976) are also given in Table 1.

Pyroxenes: Thirty grains of augite from ten samples were analysed using the microprobe and representative analyses are given in Table 2. Well developed crystals, indicating equilibrium crystallisation, with minimal alteration along the cleavage and fractures were chosen for analysis. As no chemical zoning was detected, areas for analysis were generally selected in the core of the grains to avoid any incipient alteration. Concentrations of ferric iron were calculated by the method of Papike *et al.*(1974). These samples show a narrow range in composition and are generally enriched in aluminum (3.5% to 8.1% Al_2O_3) and titanium (0.99% to 2.09% TiO_2). The chromium content is generally low (0.13 to 0.32 %.Cr_2O_3) but in the Al and Ti poor samples, it is as high as 0.8%.

Amphibole: Eighteen grains of amphibole from seven samples were also analysed with the microprobe. In two samples (8932 and 3694) both augite and amphibole are present as the relict phases. In others, amphibole is the only relict mineral. Representative analyses are given in Table 3. All samples are enriched in titanium with TiO_2 ranging from 4.5% to 5.95%, corresponding to 0.51 - 0.68 Ti atoms per formula unit(O=23). According to the nomenclature of amphiboles proposed by Leake (1978), they are classified as kaersutites.

---

[1]Complete set of analyses are given in appendix II.

Table 1.Representative Basalt Analyses[1,2]

No.	1700	110	2559	2551	1893[3]	3459	2715[3]	3458	5558[4]	5613[4]
SiO_2	49.49	50.68	49.07	50.58	50.46	47.61	50.10	54.50	50.40	48.80
Al_2O_3	15.21	14.27	15.77	14.44	14.48	14.13	15.79	15.13	14.40	13.44
Fe_2O_3	11.84	11.43	10.68	12.24	11.63	14.99	11.94	10.85	12.70	13.96
MgO	7.92	7.31	6.45	7.48	7.05	8.96	6.81	5.36	7.75	7.77
CaO	10.39	9.90	13.94	10.25	10.13	9.61	10.13	8.16	8.48	9.86
Na_2O	3.07	4.20	1.87	2.71	3.92	2.04	2.69	3.68	3.80	3.63
K_2O	0.06	0.05	0.04	0.08	0.04	0.04	0.22	0.04	0.37	0.08
TiO_2	1.62	1.76	1.77	1.78	1.88	2.18	1.90	1.90	1.72	2.05
MnO	0.19	0.18	0.18	0.22	0.19	0.23	0.19	0.19	0.20	0.21
P_2O_5	0.20	0.21	0.23	0.22	0.21	0.20	0.22	0.19	0.19	0.21
Zr[5]	123	130	126	119	132	123	129	130	169	156

[1] in percent by weight
[2] recalculated to 100% on a volatile-free basis
[3] kaersutite-bearing
[4] from Hall-Bayer (1976)
[5] in ppm

Table 2. Representative Pyroxene Analyses[1]

No.	4592	4962	1392	2241	2242	7151	7152	8932	1941	1991
SiO_2	49.55	48.27	50.57	51.20	49.44	48.62	47.66	46.04	48.07	51.62
Al_2O_3	5.18	5.54	6.37	3.51	4.25	5.71	5.92	8.10	5.42	2.48
TiO_2	1.25	1.44	0.44	0.99	1.28	1.68	2.09	2.55	1.82	0.68
FeO	7.27	7.14	7.19	8.76	9.36	9.05	8.98	9.52	9.93	8.52
Fe_2O_3	0.87	1.22	0.0	0.0	0.0	0.0	0.0	0.0	0.06	0.0
MgO	14.47	13.97	13.76	15.83	14.47	14.04	13.42	11.85	13.17	17.08
CaO	21.20	20.97	21.19	19.15	19.41	19.73	20.15	20.52	19.91	17.74
Cr_2O_3	0.32	0.21	0.19	0.23	0.13	0.18	0.14	0.16	0.17	0.20
MnO	0.16	0.13	0.16	0.18	0.18	0.14	0.15	0.17	0.21	0.21
Na_2O	bdl	bdl	bdl	bdl	bdl	bdl	bdl	bdl	bdl	bdl
Total	100.1	98.76	99.87	99.35	98.51	99.16	98.51	98.77	98.76	98.53
No. Of Cations On The Basis Of 6 Oxygens										
Si	1.84	1.83	1.87	1.90	1.87	1.83	1.81	1.75	1.82	1.93
Al	0.23	0.25	0.28	0.15	0.19	0.25	0.26	0.36	0.24	0.11
Ti	0.03	0.04	0.01	0.03	0.04	0.05	0.06	0.07	0.05	0.02
Fe^{2+}	0.23	0.23	0.22	0.27	0.30	0.28	0.28	0.30	0.32	0.27
Fe^{3+}	0.02	0.03	0.0	0.0	0.0	0.0	0.0	0.0	0.00	0.0
Mg	0.80	0.79	0.76	0.87	0.81	0.79	0.76	0.67	0.74	0.95
Ca	0.84	0.85	0.84	0.76	0.79	0.79	0.82	0.83	0.81	0.71
Cr	0.01	0.01	0.01	0.01	0.00	0.01	0.00	0.00	0.01	0.01
Mn	0.01	0.00	0.00	0.01	0.01	0.00	0.00	0.01	0.01	0.01
Wo	45.11	45.61	46.12	39.88	41.44	42.59	43.97	46.18	43.31	36.84
Fs	12.07	12.12	12.22	14.25	15.60	15.25	15.29	16.72	16.86	13.81
En	42.81	42.27	41.66	45.86	42.96	42.16	40.74	37.10	39.84	49.34

[1] in percent by weight
bdl: below detection limit

Table 3. Representative Amphibole Analyses [1]

No.	3466	4662	2715	2712	1893	8932	3413	3410	3694	3861
SiO_2	40.99	40.36	42.06	41.91	39.55	39.13	40.42	39.72	40.49	44.87
Al_2O_3	11.24	12.16	11.24	10.65	14.05	14.47	10.82	12.00	12.12	12.44
TiO_2	4.51	4.63	4.68	5.13	4.44	4.66	5.95	5.20	4.60	3.42
FeO	17.33	15.44	16.75	16.11	15.62	16.01	16.59	14.76	11.66	14.62
MgO	10.77	11.66	16.11	10.82	10.37	10.03	10.21	11.20	13.57	8.98
CaO	9.84	10.22	10.82	10.90	10.64	10.88	10.56	10.65	11.08	9.38
MnO	0.24	0.19	10.90	0.24	0.20	0.21	0.24	0.22	0.25	0.17
Na_2O	2.40	2.54	0.24	2.18	2.74	2.56	2.42	2.68	3.70	4.70
K_2O	0.08	0.11	0.09	0.09	bdl	0.07	0.19	0.15	0.16	bdl
H_2O	2.60	2.68	2.18	1.96	2.38	1.99	2.60	3.40	2.38	1.42
No. Of Cations On The Basis Of 23 Oxygens										
Si	6.19	6.06	5.64	6.26	5.93	5.86	6.12	6.02	6.01	6.56
Al	2.00	2.15	1.78	1.87	2.48	2.56	1.93	2.14	2.12	2.15
Ti	0.51	0.52	0.47	0.58	0.50	0.52	0.68	0.59	0.51	0.38
Fe^{2+}	2.19	1.94	1.88	2.01	1.96	2.01	2.10	1.87	1.45	1.79
Mg	2.42	2.61	3.22	2.41	2.32	2.24	2.30	2.53	3.00	1.96
Ca	1.59	1.64	1.55	1.74	1.71	1.75	1.71	1.73	1.76	1.47
Mn	0.03	0.02	1.24	0.03	0.03	0.03	0.03	0.03	0.03	0.02
Na	0.70	0.74	0.06	0.63	0.80	0.74	0.71	0.79	1.06	1.33
K	0.02	0.02	0.37	0.02	0.0	0.01	0.04	0.03	0.03	0.00

[1] in percent by weight
[2] the total of all oxides including water is 100%
bdl: below detection limit

F. Discussion

Initial composition of the volcanic rocks

Hall-Bayer (1976) classified the basaltic rocks of the Fennell Formation as abyssal tholeiites, in part komatiites, on the basis of major, minor and trace element geochemistry. The major-element, whole-rock compositions of Fennell Formation basalts of this study (Table 1) are also broadly similar to those of low-K abyssal tholeiites (Wilkinson, 1982). However, absence of olivine and dominance of augite as a phenocryst phase in these rocks contrasts with present-day, abyssal tholeiites in which olivine forms a significant part of the phenocryst assemblage and augite is rare (Bryan, 1979; Miyashiro *et al.*, 1969).

The apparent similarity of major element compositions to abyssal tholeiites is probably due to chemical changes during alteration (Hart, 1969; Hart, 1970; Hart *et al.*, 1974 Humphris and Thompson, 1978a). The degree of chemical modification during alteration depends on the relative mobility of the elements which is influenced by temperature, water to rock ratio and composition and crystallinity of the rock (Hajash and Chandler, 1981). For a meaningful interpretation of the major element composition, it is important to examine the nature of alteration and its effects on the composition of these rocks.

As suggested by the existence of pillow structures and associated marine sediments, it is likely that the Fennell Formation rocks were formed in a submarine environment and consequently, suffered alteration through seawater - rock interaction. The behaviour of elements during alteration of ocean basalts has been studied by many authors, both at low-temperature (Hart, 1969; Hart *et al.*, 1974; Scarfe and Smith 1977) and high-temperature (Bishoff and Dickson, 1975; Hajash, 1975; Mottl and Holland, 1978; Humphris and Thompson, 1978a). According to these studies, the mobility of elements changes significantly as a function of the temperature of alteration. Furthermore, it is noted that an element may be either added or removed from the rocks depending on the temperature of alteration (Hajash and Archer, 1981). The rocks of the present study are from the vicinity of the Chu Chua ore deposit and represent both the hangingwall and footwall sections. These rocks would have suffered alteration under varying conditions of temperature as the hangingwall rocks will not be subjected to the

high temperature hydrothermal alteration during ore formation. Despite this variability in the alteration regimes, the hangingwall and footwall rocks are remarkably similar in their petrographical, mineralogical, and chemical characteristics. Thus, the uniformly low potassium content in the basaltic rocks of the Fennell Formation (see Table 1), for example, may be a result of the combined effects of the low temperature sea-floor weathering, higher temperature hydrothermal alteration, and the low-grade regional metamorphism. This suggests that the apparent similarity in major element composition of the Fennell Formation basalts to abyssal tholeiites may be fortuitous.

As the crystallisation sequence and composition of the phenocrysts are characteristic of the bulk composition, relict minerals in altered rocks can be reliable indicators of magmatic composition of the rocks. Relict microphenocrysts of kaersutite, clinopyroxene and Fe-Ti oxides, commonly present in Fennell Formation basalts, provide useful criteria for this purpose as discussed below.

Kaersutite has a very restricted occurrence in basaltic rocks and is reported only from alkalic basalts or mantle xenocrysts in alkaline rocks (Aoki, 1963; Gunn, 1972; Brandle, 1974; Wilkinson, 1961; Kesson and Price, 1972). Cawthorn (1976a, b) argues that only an alkalic magma, because of its high alkali and titanium contents, can precipitate kaersutite as a stable liquidus phase. This suggests that the kaersutite-bearing rocks in the Fennell Formation are alkalic basalts.

The composition of crystallising clinopyroxenes is also greatly affected by the bulk composition of the magma. LeBas (1962) suggested that the Ca-content of calcic clinopyroxenes increases with the total alkali content of the magma and that the clinopyroxene in alkali basalts are generally more calcic than those in tholeiitic basalts. Fodor *et al.*, (1975) observed similar trends in clinopyroxenes from Hawaiian basalts and noted that the Ca content increases from tholeiitic to nephelinitic suites. Within the alkalic suite, the wollastonite component varies from Wo_{42} in alkali basalts to Wo_{48} in mugearites. The clinopyroxenes analysed in this study are all calcic augites with the wollastonite component ranging between Wo_{42} and Wo_{44} (Table 2) and ferrosilite component less than Fs_{17}. These compositions are plotted on the conventional pyroxene quadrilateral in Figure 2.

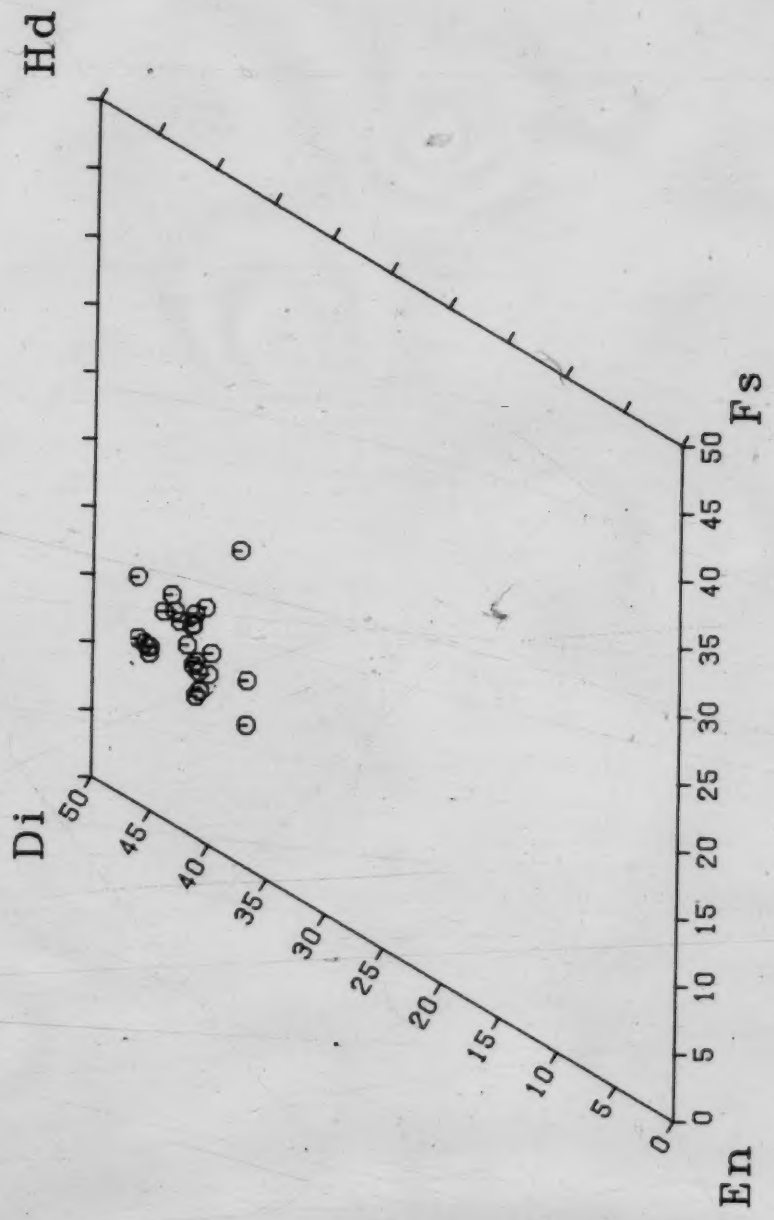

Figure 2. Quadrilateral plot of composition of augites from basalts at Chu Chua

Kushiro (1960, 1972), LeBas (1962), Carmichael *et al.* (1970) and Gupta *et al.* (1973) have studied the relation between the silica content of the magma and the Si, Al and Ti contents of clinopyroxene. These authors suggest that with an increase in the silica content of the magma, the Si content of clinopyroxene increases and the Al – Ti content decreases. Carmichael *et al.*(1974) suggest that, in general, the Al_2O_3 content of a clinopyroxene in a tholeiitic basalt is less than 2.5% and the TiO_2 content varies from 0.9 to 1.1%. The Al_2O_3 and TiO_2 contents of all augites, except 1991, analysed in this study are more than 3.5% and 0.9% respectively (Table 2) and vary antipathetically with the Si content. The relatively lower Al and Ti contents in sample 1991 may be due to minor variations in the silica activity of the magma.

Statistical analyses of clinopyroxene compositions from altered and fresh basaltic rocks (Nisbet and Pearce, 1977; Leterrier *et al.*, 1982; Schweitzer *et al.*, 1979) indicate that the pyroxene compositions can be used for discriminating between alkalic and tholeiitic basalts. The differences between clinopyroxenes from alkalic and tholeiitic basalts are more pronounced in the compositions of the phenocrysts because the groundmass pyroxenes, crystallising in the later stages of the cooling of a magma, inherit the composition of the residual melt (Smith and Lindsley, 1971). Therefore, the groundmass pyroxenes are much less sensitive to variations in bulk composition than the phenocrysts. Nisbet and Pearce (1977), using groundmass pyroxenes, suggested that discrimination between alkalic and tholeiitic rocks based on clinopyroxene compositions are not reliable. However, their conclusions are not widely applicable as the groundmass pyroxenes may not represent the true composition of the magma (Fodor *et al.*, 1975; Letterier *et al.*, 1982). Using phenocryst compositions, Leterrier *et al.* (1982) recently suggested that the alkali basalts can be distinguished from the tholeiitic basalts on the basis of the Ca, Na and Ti contents of their clinopyroxenes. The cation proportions of Ca+Na and Ti of augites of this study are plotted in Figure 3. Augites from kaersutite-bearing rocks of the Fennell Formation lie in the alkali basalt field and those from kaersutite-free rocks generally plot in the overlap region of the alkalic and tholeiitic basalt fields of Leterrier *et al.* (1982). Comparing clinopyroxene compositions from deep-sea basalts, Schewitzer *et al.*, (1979) delineated compositional fields occupied by clinopyroxenes from tholeiitic and alkali basalts. Their data base included clinopyroxenes

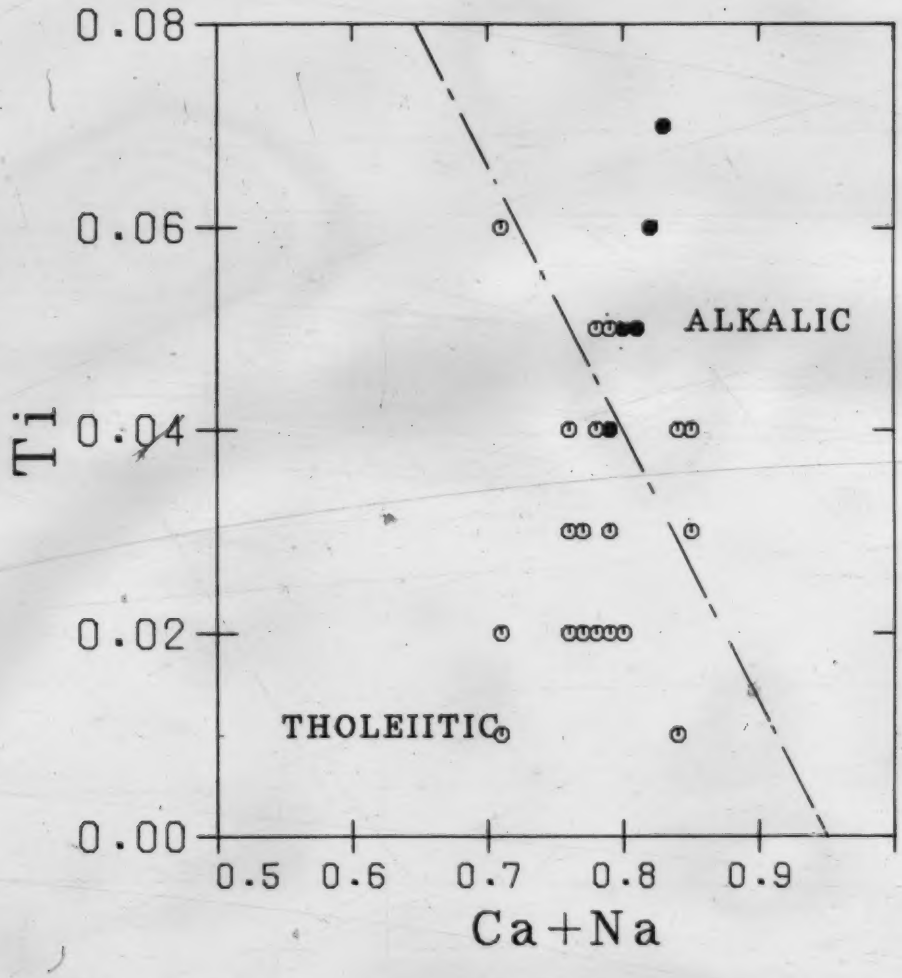

Figure 3. Ca+Na vs Ti (cation proportion) contents of Augites in basalts from Chu Chua. The alkalic and tholeiitic basalt fields and the dividing line are as proposed by Letterier *et al.* (1982). The solid symbols represent kaersutite-bearing basalts and the hollow symbols, kaersutite-free basalts.

of abyssal tholeiites and alkali basalts from seamounts but they did not specify whether groundmass or phenocryst compositions were used. On the Fe^{2+} / Mg + Fe^{2+} (cation proportion) diagram proposed by these authors, augite compositions from this study again display the alkalic and transitional nature of their host rocks (Fig.4). Based on the above discussion, it is concluded that the Fennel Formation consists of altered, alkalic and transitional basalts.

The occurrence and timing of crystallisation of the Fe – Ti oxides can also be used to identify the magmatic composition of the altered, volcanic rocks. Crystallisation of iron–titanium oxides depends on the oxidation state of the magma. Carmichael *et al.* (1974) noted that temperature, fugacity of oxygen and the alkali content of the magma are the major factors which influence the oxidation state of silicate melts and that for terrestrial magmas, it can be directly related to the total alkali content. Recently, Sack *et al.* (1980) suggested that alkalic magmas are more oxidised than tholeiitic magmas which tends to stabilise the Fe – Ti oxide minerals in the phenocryst stage of crystallisation of an alkali magma. On the other hand, the oxidation state in a tholeiitic magma is generally quite low so that Fe – Ti oxides crystallise only in the groundmass. The presence of microphenocrysts of titanomagnetite in Fennell Formation basalts indicates alkalic affinities of the rocks which is consistent with the relict mineral chemistry.

Another approach for the identification of the magmatic composition of altered rocks is to use the 'immobile' elements such as Ti, Y, Zr and P as discriminants (Pearce and Cann, 1971,1973; Floyd and Winchester, 1975). This approach has been frequently used (e.g. Bevins, 1981; Grenne and Roberts 1980) to identify the magmatic composition and tectonic setting of altered volcanic rocks. Floyd and Winchester (1975) suggested that the Ti – Zr, Ti – Zr/P_2O_5, and Zr / P_2O_5 diagrams can be useful in discriminating between alkalic and tholeiitic basalts. On these diagrams (Figs.5 – 7) the Fennell Formation rocks, including the kaersutite–bearing rocks, plot in the tholeiitic basalt field. This is inconsistent with the alkalic and transitional nature of these basalts suggested by mineralogical characteristics.

There could be two possible explanations for this observation. The first possibility is that the trace elements believed to be 'immobile' may be mobile in certain conditions so that original concentrations are not preserved (Hynes, 1980; Finlow–Bates

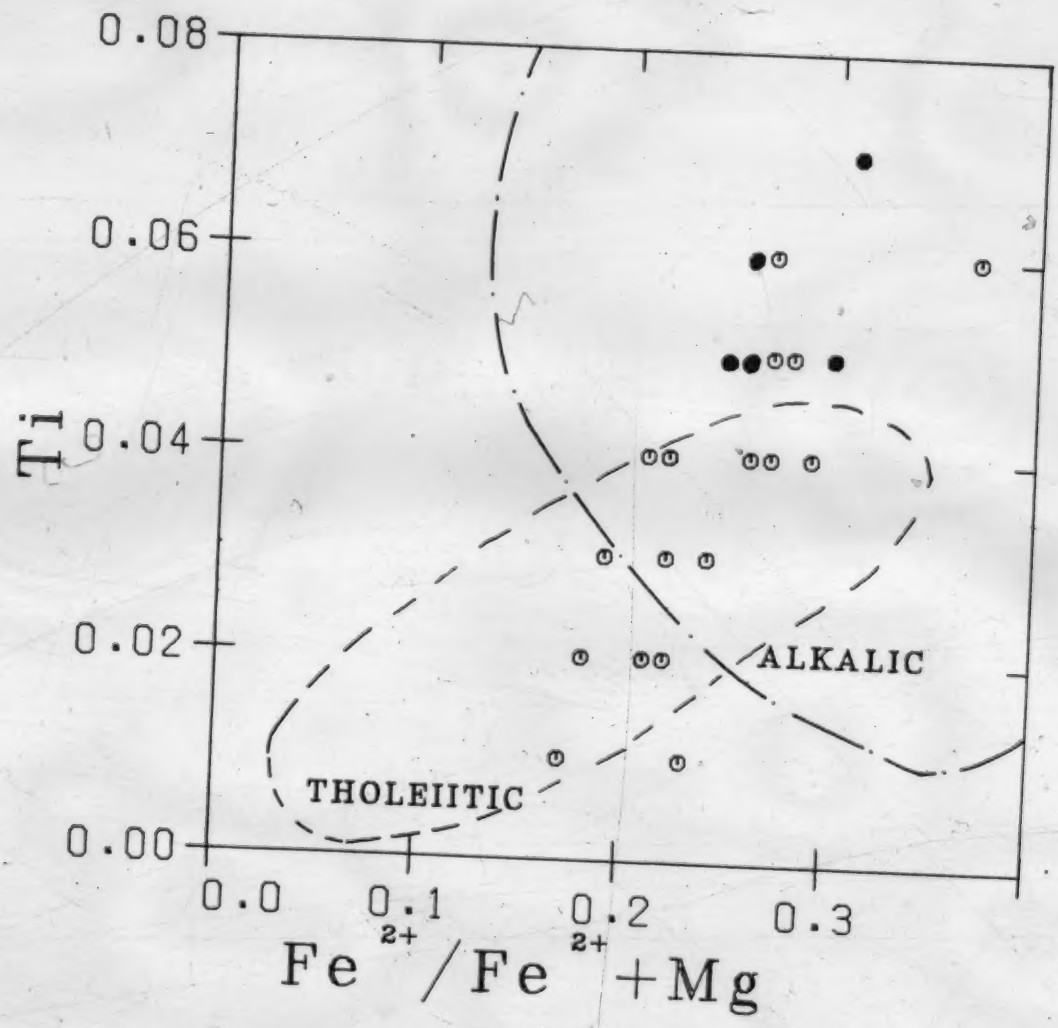

Figure 4. $Fe^{2+}/(Fe^{2+} + Mg^{2+})$ content of augites. The alkalic and tholeiitic basalt fields are those of Schweitzer *et al.* (1979). Symbols are as in Figure 4.

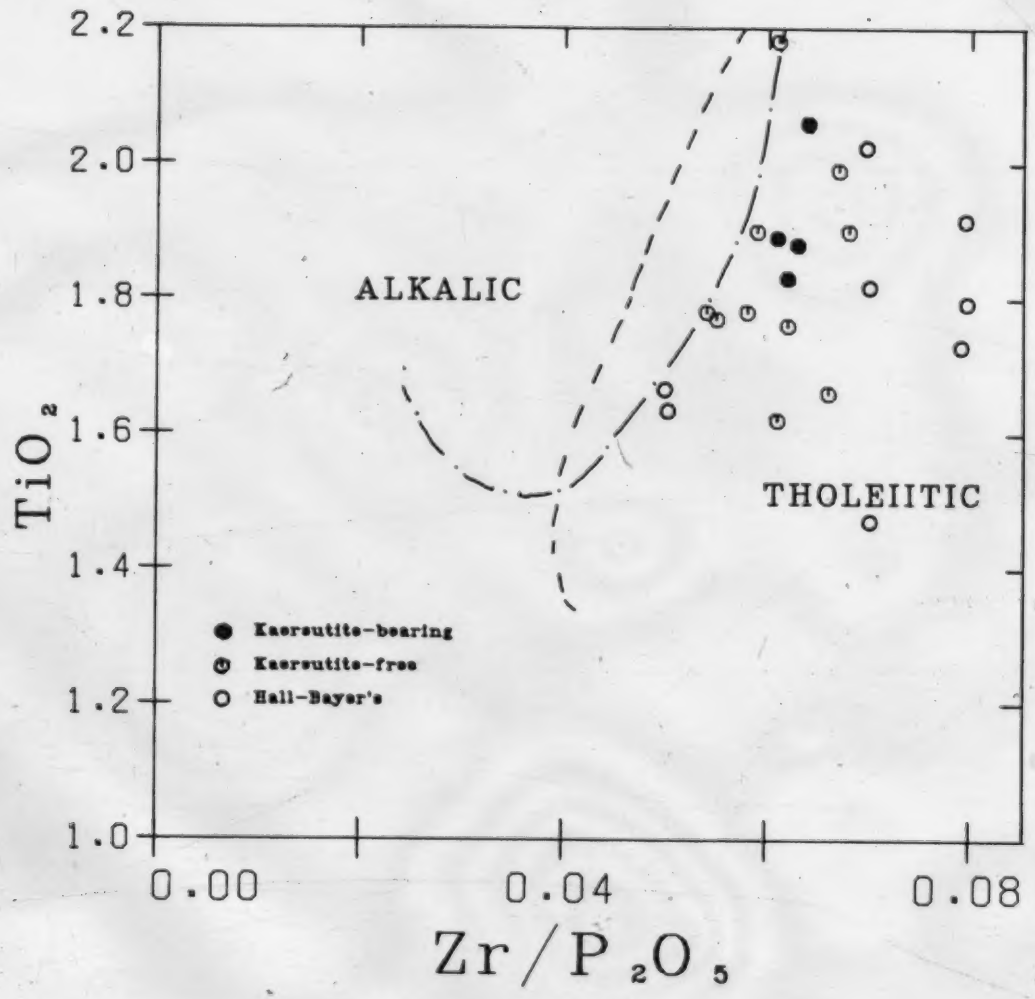

Figure 5. Ti vs Zr/P_2O_5 diagram of Floyd and Winchester (1975) for discriminating between alkalic and tholeiitic basalts. The Fennell Formation basalts all plot in the tholeiitic field.

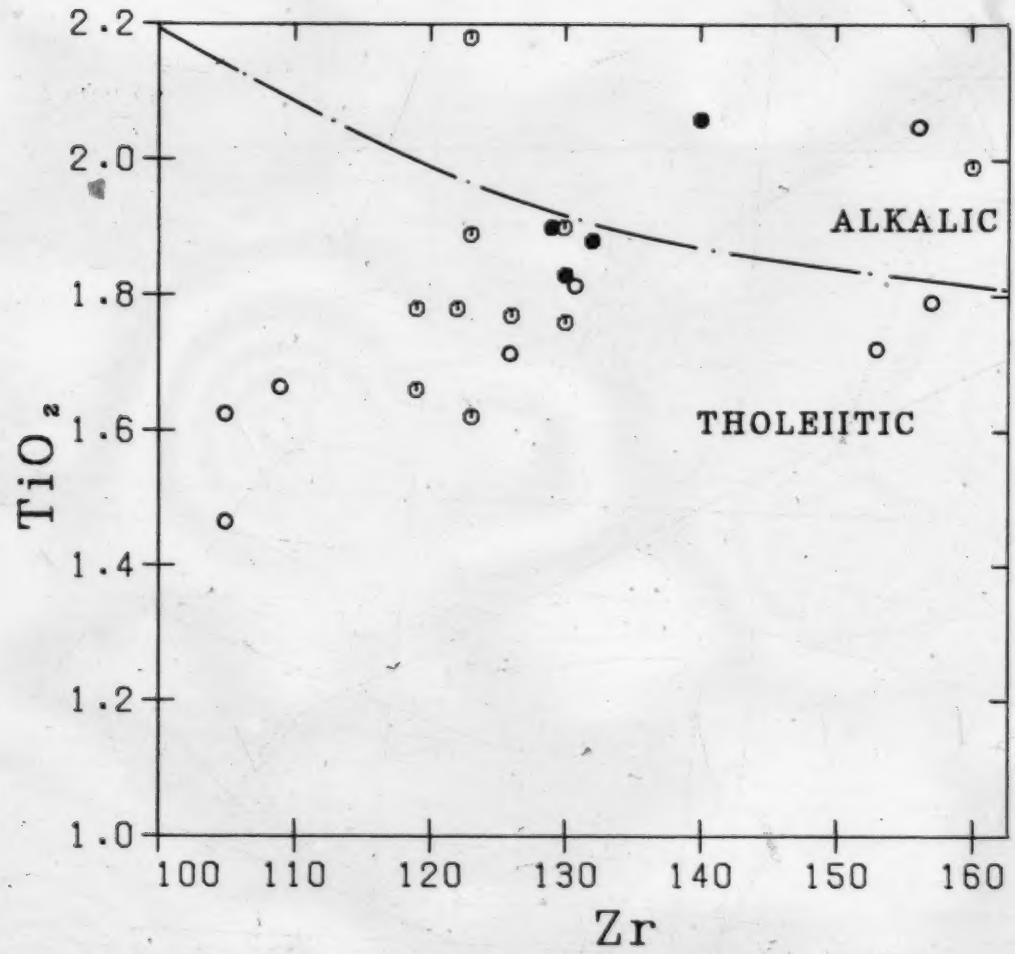

Figure 6. Ti vs Zr diagram of Floyd and Winchester (1975) The Fennell Formation basalts lie mostly in the tholeiitic field. Symbols as in Figure 6.

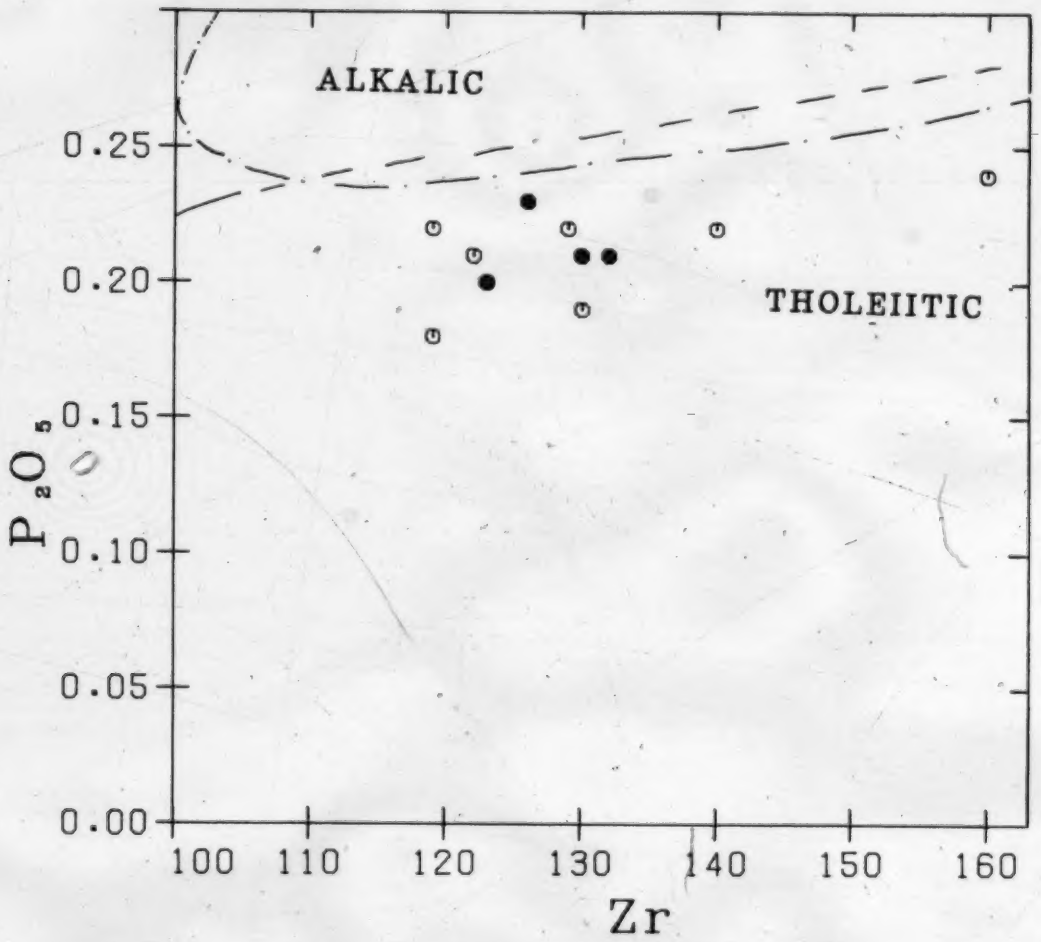

Figure 7. Compositions of Fennell Formation basalts in the Zr vs P_2O_5 discrimination diagram. The Fennell Formation basalts again plot in the tholeiitic field. symbols and fields as in Figure 6.

and Stumfl, 1981). Although the rocks of this study are from the vicinity of an ore deposit, any abnormal patterns of elemental behaviour compared with barren areas seem unlikely because data from the barren parts of this Formation (Hall-Bayer, 1976) show similar values (Table 1) and lie in the tholeiitic basalt field in Figures 5 and 6. The Ti, Zr and P contents in the rocks of the Fennell Formation are very similar (Table 1) and on do not show any significant linear correlation. This indicates that either these elements were unaffected during alteration and metamorphism or have been peculiarly affected to lose their linear relationships (Pearce and Cann, 1973; Bevins, 1981). Therefore, the mobility or immobility of these elements in the Chu Chua area cannot be conclusively proved. The second explanation could be that the diagrams based on these elements do not provide a clear discriminantion between rocks of different composition or tectonic setting. Wood *et al*. (1979) and Holm (1982) suggested that discrimination between volcanic rocks from various tectonic settings, based only on the immobile element compositions, may not be unambiguous in all cases. It is possible that similar ambiguities prevail in discriminating between rocks of different chemical compostions. Because the most likely alkalic (kaersutite-bearing) rocks of this study lie in the tholeiitic basalt field and cannot be distinguished from others, this could be a plausible explanation. However, it is difficult to choose between the two possibilities as both of them may have contributed to the present situation in which the alkalic rocks of this study have the so called 'immobile element signatures' similar to tholeiitic basalts.

In summary, attempts to identify the magmatic composition of altered volcanic rocks of this study based only on the concentrations of the major, minor and trace element compositions are ambiguous. The petrographical and mineralogical study of the relict minerals appear to provide more reliable evidence for this purpose. Based on these criteria, it is suggested that the basaltic rocks of the Fennell Formation are alkalic and transitional in character.

Tectonic Setting

Hall-Bayer(1976) and Monger(1977) suggested that the Fennell Formation rocks are abyssal tholeiites representing part of the ancient oceanic crust. The presence of alkalic rocks in this Formation, however, raises doubts about this interpretation. Alkalic rocks are believed to be characteristic of off-axis and mid-plate volcanic centres such

as ocean islands, seamounts, back-arc basins, fracture zones and continental rifts (eg. Gast, 1968; Melson and Thompson, 1972).

Occurrence of interbedded marine chert and pillow structures in the Fennell Formation eliminates any possibility of a continental origin. Alkali basalts from oceanic tectonic settings have very few geochemical differences. However, the associated tholeiitic phase is noticeably different in various tectonic regimes. Tholeiitic basalts in the back-arc basins and fracture zones are very similar to abyssal tholeiites and geochemically distinguishable from those in ocean islands (Chayes, 1964; McDonald and Katsura, 1964; Pearce and Cann, 1973; Dick, 1982). The transitional basalts of the Fennell Formation are more similar to ocean island tholeiites in their petrographic and mineralogical characteristics than to the abyssal tholeiites (Miyashiro *et al.*, 1969; Bryan, 1979).

An important geochemical difference in basalts from various tectonic settings is seen in their lead isotopic compositions (Tatsumoto, 1978; Sun, 1980). Sun(1980) pointed out that in general the ocean island leads are more radiogenic than MORB leads and, on a $^{207}Pb/^{206}Pb$ diagram, typically lie along a straight line having a slope of nearly 0.1. The lead isotopic compositions of the Fennell Formation basalts are given in Table 4 and are plotted in Figure 8. Lead isotope data from MORBs and Gough Islands (Sun 1980) are also plotted in this figure. Two features of the Fennel Formation basalts are apparent from this diagram: first, they lie along a straight line having a slope of 0.096; second, they are more radiogenic than typical MORBs and are similar to basalts from the Gough islands. This indicates that the tectonic environment of formation of the Fennell Formation rocks was, most likely, similar to present day ocean islands or seamounts.

Table 4. Lead Isotopic Compositions Of Fennell Formation Basalts

Sample No.	$^{206}Pb/^{204}Pb$	$^{207}Pb/^{204}Pb$	$^{208}Pb/^{204}Pb$
1893	36.92	17.12	38.32
3893	28.16	16.55	38.22
2551	20.40	15.79	38.06
1700	18.52	15.59	37.99
110	18.17	15.57	37.79
3459	18.74	15.61	37.92

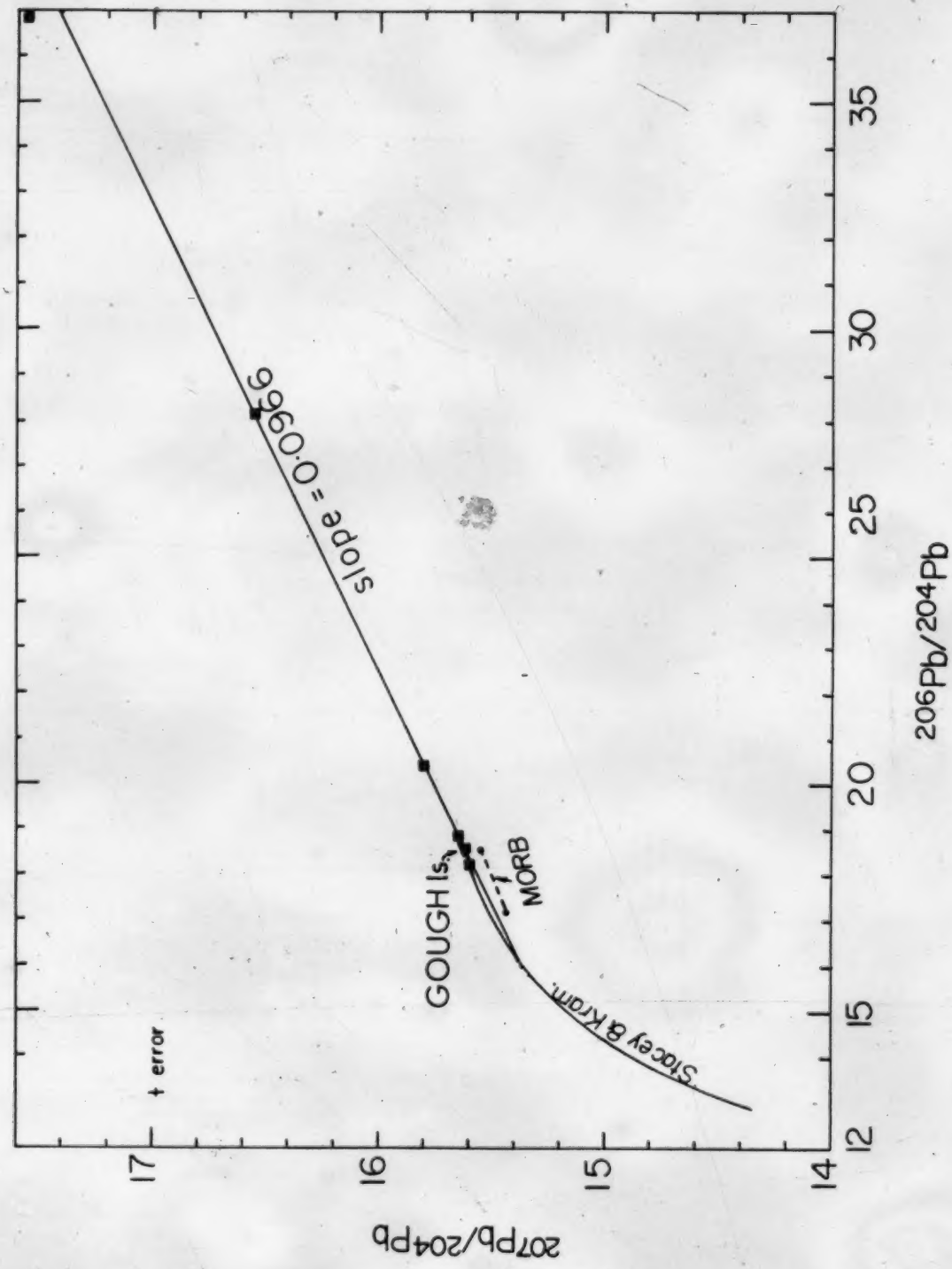

Figure 8. Lead isotopic composition of Fennell Formation basalts from Chu Chua

III. Conclusions

The phyric and aphyric basalts of the Fennell Formation in south-central British Columbia have suffered low greenschist facies metamorphism. Primary igneous textures and microphenocrysts of augite and kaersutite have survived this metamorphism and are commonly present. A characteristic petrographic feature of these basalts is the dominance of augite as a phenocryst phase, and is dissimilar to abyssal tholeiites, although the Fennell Formation has previously been considered a part of ancient oceanic crust.

Occurrence of microphenocrysts of kaersutite and Fe – Ti oxide minerals suggests that the Fennell Formation basalts were originally of alkalic composition. The composition of relict microphenocrysts of augite from kaersutite-bearing rocks is consistent with this observation and is similar to the composition of augites from alkalic basalts. Composition of augite in kaersutite-free rocks indicate a transitional character of their host basalts. On the basis of these criteria, it is suggested that the volcanic rocks of the Fennell Formation consist of altered, alkalic and transitional basalts.

The alkalic, kaersutite-bearing, and transitional rocks of this study plot in the tholeiitic basalt field on conventional Ti – Zr and Ti – Zr/P_2O_5 immobile element discrimination diagrams. It is, therefore, suggested that caution must be excercised when classifying altered rocks solely on the basis of their minor and trace element geochemistry. The lead isotopic compositions of these basalts are more radiogenic than typical mid-ocean ridge basalts and are similar to those of the basalts from Gough island. Based on this observation, the petrographic characteristics and the presence of alkalic basalts, it is suggested that the rocks of the Fennell Formation were formed in a tectonic environment similar to present-day ocean islands and seamounts.

IV. Geochemistry of the Chu Chua Massive Sulfide Deposit, British Columbia

A. Introduction

The Chu Chua massive sulfide deposit is located approximately 100Km north of Kamloops, British Columbia (Fig.2). It consists of cupriferrous iron sulfides with nearly 2 million tons of 2% copper, 0.4% zinc, 0.4 grams/tonne gold, 8 grams /tonne silver and trace amounts of tin (McMillan, 1979). The deposit occurs in the alkalic and transitional basalts of the upper Paleozoic Fennell Formation which were formed in an ocean island tectonic setting (Aggarwal, 1982). The Chu Chua deposit differs from other known mineral occurrences in the region, most of which are in felsic volcanic rocks (Vollo, 1981). McMillan (1980) and Vollo (1981) have suggested that this is a typical volcanic exhalative deposit in tholeiitic rocks, akin to the Cyprus copper deposits. The composition and tectonic setting of the host rocks and the occurrence of massive silicic, talc and talc–magnetite bodies in the footwall, however, distinguish the Chu Chua deposit from other volcanogenic massive sulfide deposits.

The object of this study is to develop a genetic model for the Chu Chua deposit, based on the geological and geochemical features of the ore and the wall rocks together with thermodynamic considerations of the stabilities of pertinent minerals. It will be shown that the massive silicic and talc rocks associated with the deposit are primary chemical precipitates and may provide useful exploration criteria for massive sulfides in similar terrains.

B. Local Geology

The Chu Chua deposit occurs on the western limb of the Chu Chua anticline in the upper division of the Fennell Formation (Fig.9). Preto (1979) suggests that rocks in the Chu Chua area dip steeply to the west but have not been overturned. This is consistent with the results of this study as will be discussed later. The deposit consists of two major, eastern and western, and two minor lenticular, bodies of massive sulfides trending north – south and dipping steeply to the west with a gentle plunge towards the south (McMillan, 1980). The sulfide bodies have sharp, upper contacts with the basalts and are mostly underlain by massive silicic or talc units (Fig.10). The eastern sulfide body,

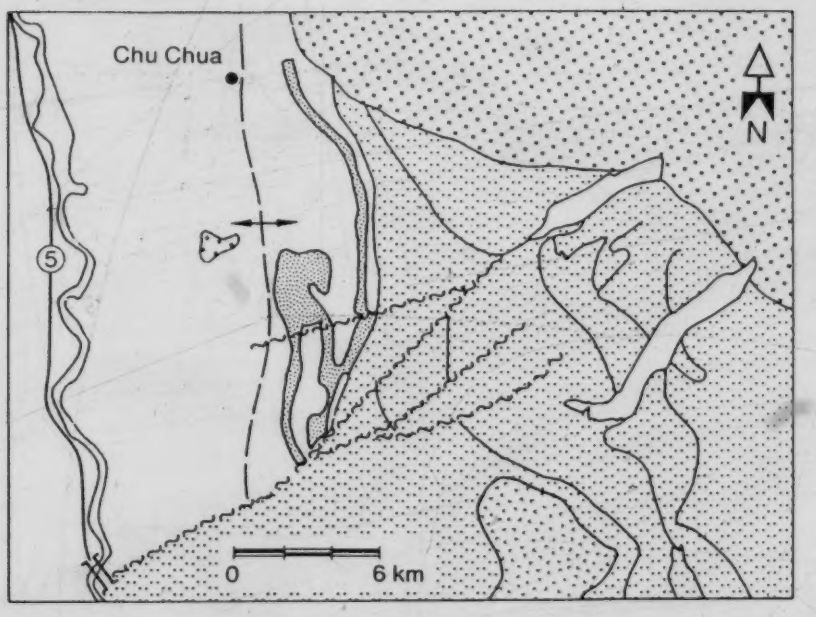

Figure 9. Geological Map of The Chu Chua Area

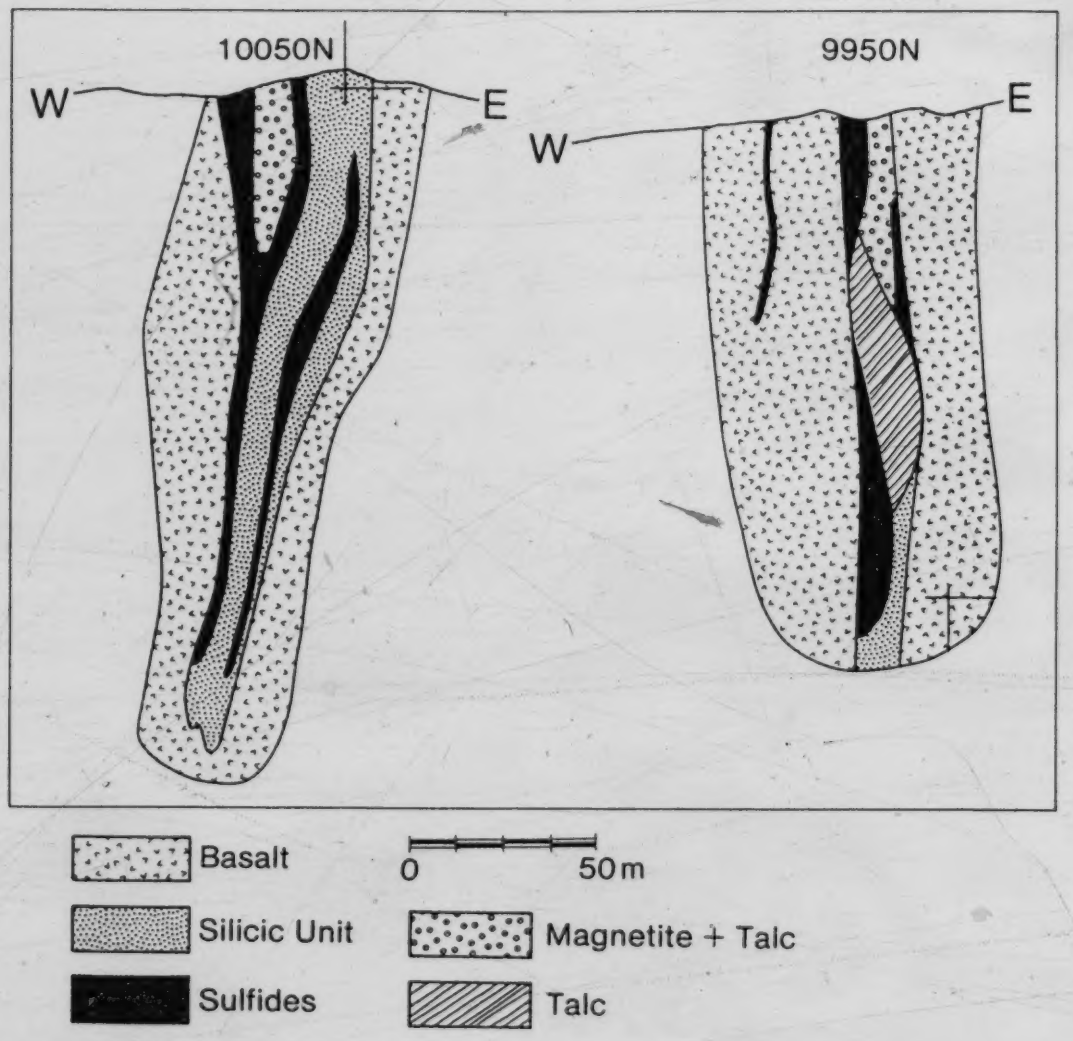

Figure 10. Vertical Sections Through The Chu Chua Ore Bodies

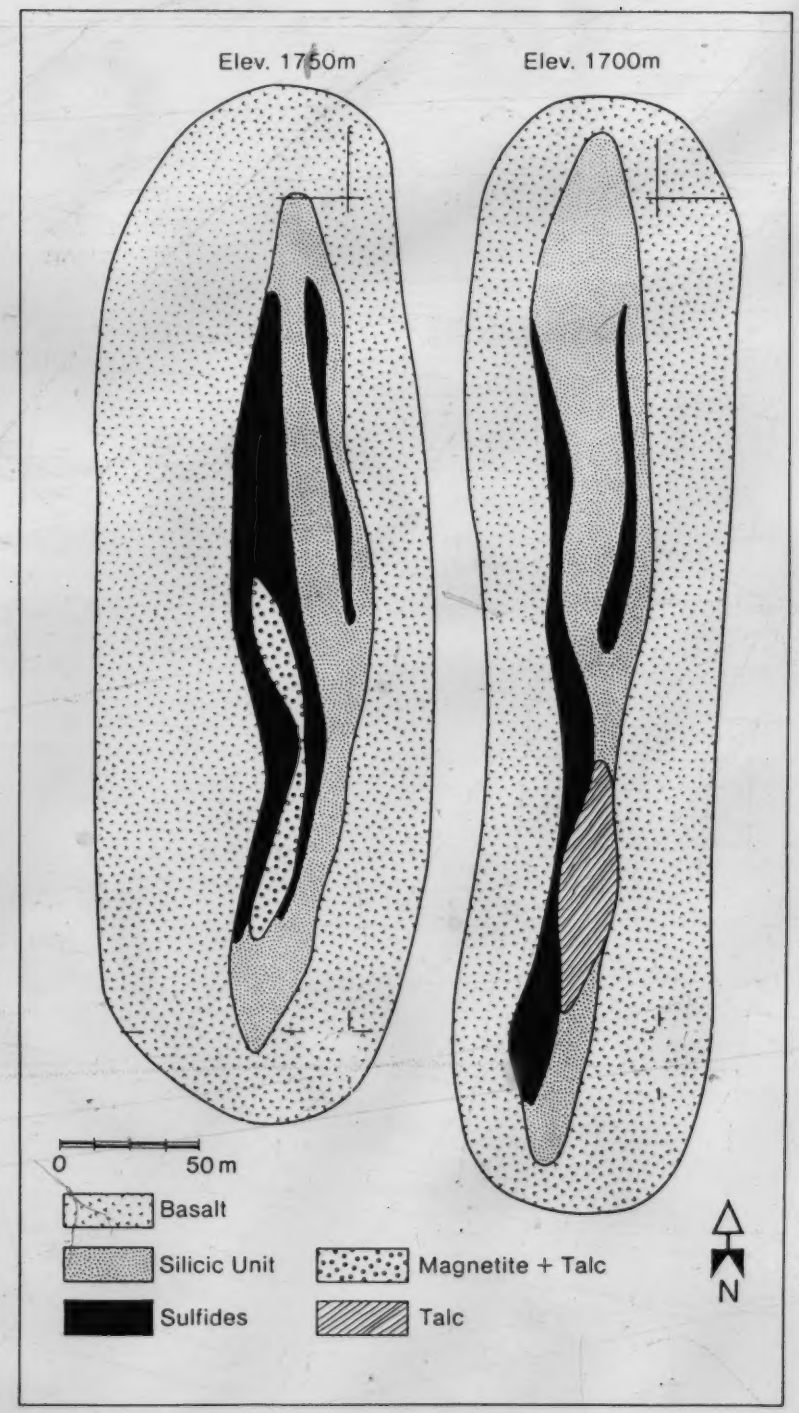

Figure 11 Horizontal Sections Through The Chu Chua Ore Bodies

however, is enclosed within the silicic unit. The contacts between the massive sulfides and the silicic unit are frequently marked by transition zones of disseminated sulfides while the massive talc unit, occurring only below the western sulfide body, is noticeably devoid of any sulfide minerals.

Sulfide bodies

The deposit has been delineated by extensive drilling and the major sulfide bodies range from 100m to 200m in length, 2 to 25m in width and have been proven to depths of 100 to 150m. Massive sulfide zones of a total width of 10 meters have recently been intersected in two holes down the plunge of the ore bodies at a depth of 300 meters. Massive talc – magnetite lenses occur partially enclosed within the sulfide sectors of both the major sulfide bodies. In the western sulfide body, the talc – magnetite lens overlies the massive talc rocks (Figs. 10, 11). The sulfide bodies are predominantly composed of pyrite and chalcopyrite with minor amounts of sphalerite, cubanite, stannite – kesterite solid solution, quartz and calcite. Magnetite generally occurs in minor amounts, associated with the sulfides, but becomes a significant phase in the vicinity of the talc–magnetite lenses.

The sulfide minerals occur in varying grain sizes and display both primary depositional, and incipient metamorphic textures. Pyrite occurs in finely crystalline masses or as coarser (0.01 to 0.05 mm), subhedral to euhedral grains. It often carries minute inclusions of chalcopyrite. The finely crystalline masses occur in colloform intergrowth with chalcopyrite and sphalerite (Plage 5), indicating little or no recrystallisation during metamorphism. In contrast, the subhedral pyrite grains have suffered grain boundary migration and show crudely defined triple–point junction textures (Plate 6). Chalcopyrite is generally interstitial to the pyrite grains, but also occurs as subhedral grains varying in size from 0.01mm to 0.1mm. Inclusions of cubanite, pyrite and sphalerite are frequently present in chalcopyrite. When etched with H_2O_2 + NH_4OH solution, coarser chalcopyrite grains display annealing twins (Plate 7) but no significant deformation twinning. Sphalerite mostly occurs in fine intergrowth with pyrite and chalcopyrite or as inclusions in chalcopyrite. Isolated, subhedral grains of sphalerite are uncommonly present and show incipient deformation twinning when etched with 47% HI solution. Stannite – kesterite solid solution, observed in one sample, is associated with

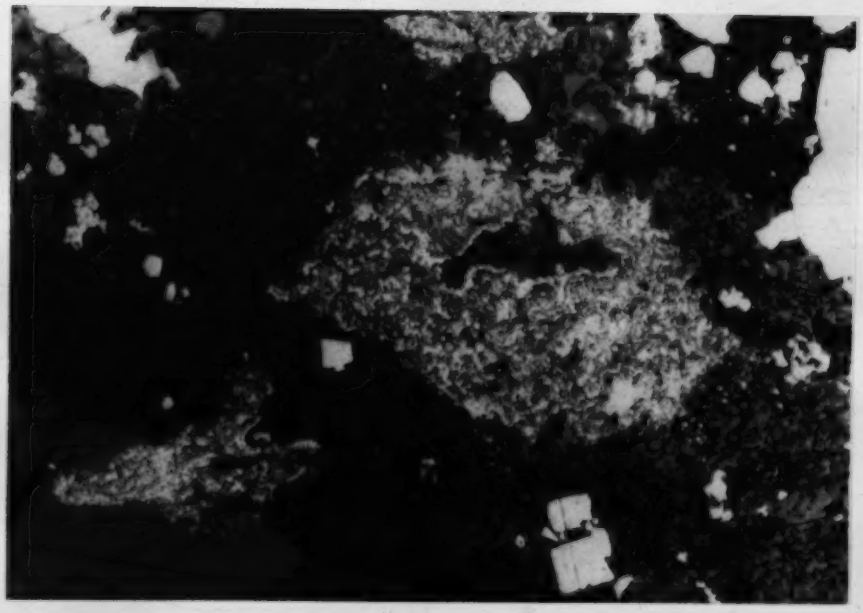

Plate 5. Fine intergrowths of Pyrite – Chalcopyrite – Sphalerite displaying colloform texture

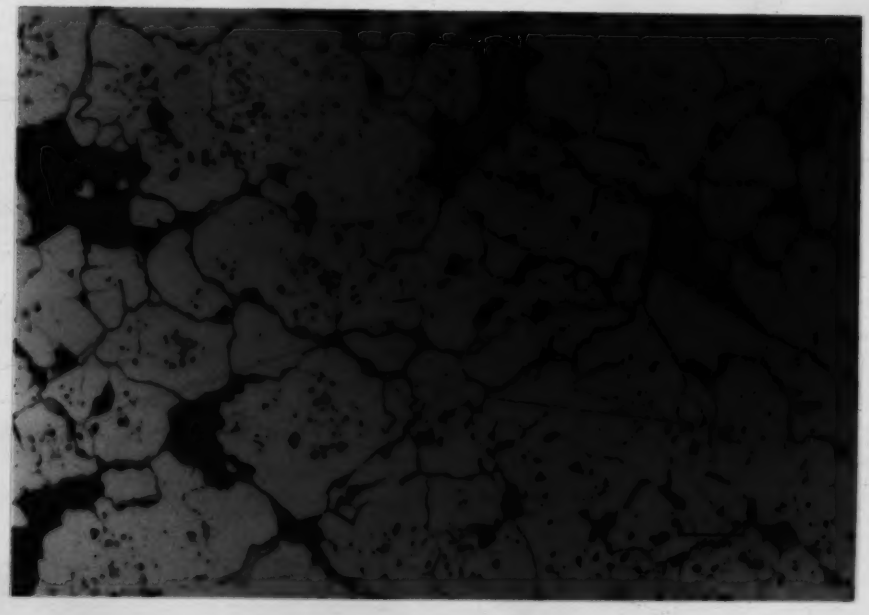

Plate 6. Subhedral pyrite grains showing triple-point junction texture

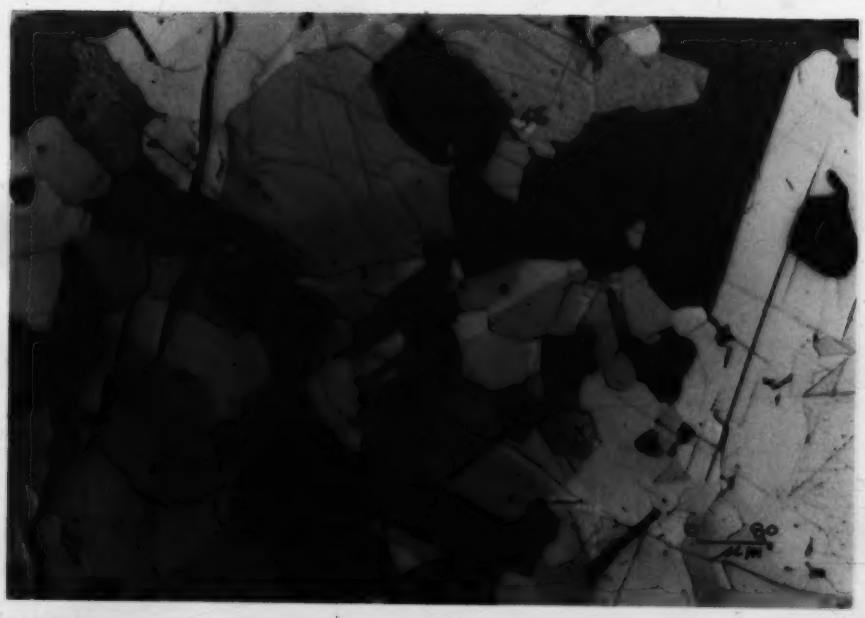

Plate 7. Annealing twins in Chalcopyrite

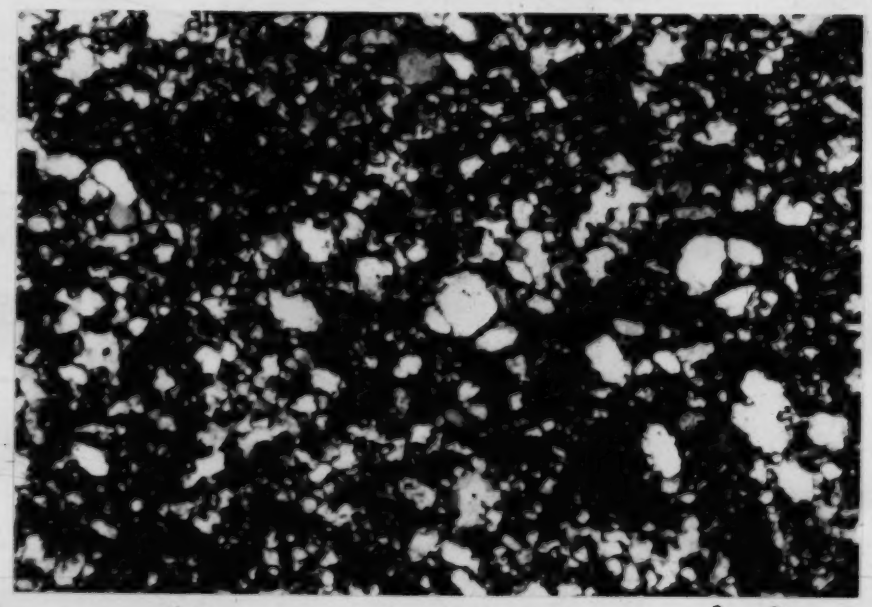

Plate 8. Fine-grained anhedral quartz in silicic unit

sphalerite and chalcopyrite. It occurs as a composite phase and does not show exsolution of Fe or Zn rich end members.

Wall rocks

The Chu Chua deposit is hosted in the massive or pillowed, phyric and aphyric basalts of the Fennell Formation. Although these basalts have suffered low greenschist facies metamorphism, their primary igneous textures are still preserved. Discrete or glomerophyric microphenocrysts of augite, albitised plagioclase and kaersutite occur in a matrix of albite, actinolite, chlorite, zoisite, sphene–leucoxene, quartz, and calcite. The whole–rock compositions of these basalts (Table 1) do not show any significant chemical differences from the hangingwall to the footwall of the deposit.

The sulfide bodies in the Chu Chua deposit are generally underlain by the silicic and the talc units which are fine–grained and massive. The rocks of the silicic unit are predominantly composed of quartz with minor amounts of phengitic mica and chlorite. Disseminated pyrite, and sometimes chalcopyrite, is commonly present. Quartz occurs as fine, anhedral grains with a mosaic texture (Plate 8). Small flakes of phengitic mica, with no preferred orientation, generally occur in the interstices of the quartz grains. These rocks do not show any replacement features such as relict or pseudomorphic minerals and partially altered basaltic textures. The whole–rock analyses of the silicic rocks (Table 5) show, on an average, 83% SiO_2 and 4% each of Al_2O_3, MgO and Fe_2O_3. The CaO, Na_2O and K_2O contents are less than 0.8%. They have very low titanium (0.2% TiO_2), phosphorous (0.02% P_2O_5) and manganese (0.2% MnO) contents. Samples 1565 and 1577 (Table 5) show slightly higher aluminum values. These samples are stratigraphically higher than others and the greater aluminium content may reflect a higher detrital component.

The talc unit has very sharp contacts with the underlying basalts and shows a general increase in the magnetite content towards its contact with the overlying sulfide body. The silicic unit is laterally adjacent and does not underlie the talc unit (Figs. 10, 11). The contacts between these two units are sharp and do not have any transition zones. The rocks of the talc unit consist essentially of talc (d_{001}=9.4 A, d_{060}= 1.52 A) and occasionally, minor amounts of magnetite. These rocks are massive and finegrained and do not show any replacement or pseudomorphic textures. The whole–rock chemical analyses of these rocks (analyaes 7 – 9, Table 5) are consistent with their monomineralic

Table 5. Whole-Rock Analyses of The Silicic and Talc Units[1,2]

No.	1116[3]	1666[3]	734[3]	3144[3]	1565[3]	1577[3]	190[4]	2500[4]	2546[4]
SiO_2	88.72	91.18	81.71	70.69	69.72	82.60	60.44	58.16	38.68
Al_2O_3	2.41	3.71	4.47	3.74	9.63	7.37	0.78	1.22	1.24
Fe_2O_3	2.62	1.52	5.68	18.12	11.97	6.11	10.54	16.55	37.87
MgO	3.51	1.68	5.80	4.42	5.77	2.96	26.39	21.72	14.13
CaO	1.21	0.49	1.25	0.37	0.81	1.88	0.73	0.09	3.17
Na_2O	0.31	0.14	0.14	0.17	0.01	0.17	0.11	0.33	0.36
K_2O	0.02	0.83	0.02	0.09	0.83	1.34	0.02	0.03	0.12
TiO_2	0.15	0.17	0.22	0.27	0.77	0.39	0.03	0.03	0.05
MnO	0.03	0.05	0.06	0.08	0.28	0.07	0.0	0.0	0.12
P_2O_5	0.04	0.02	0.04	0.02	0.42	0.10	0.02	0.03	0.04
Zr[5]	88	64	84	41	84	77	13	13	5

[1] in percent by weight
[2] recalculated to 100% on a volatile free basis
[3] silicic unit
[4] talc unit
[5] in ppm

nature. These analyses show 50% SiO_2, 10% Fe_2O_3 and 30% MgO. As in the silicic unit, the Al, Ti, Mn and P contents of these rocks are also very low.

Origin of the footwall rocks

Silicic rocks are commonly associated with volcanogenic massive sulfide deposits, for example the Kuroko, Matagami Lake and Noranda deposits, occuring either or both in the hangingwall and the footwall of the sulfides (Franklin *et al.*, 1981). Those in the footwall are thought to be the products of extensive silicification of the host rocks by the ascending hydrothermal solutions (Cathles, 1981). On the other hand, the massive cherts or tuffites overlying the sulfides are considered to be the chemically precipitated sinters in the later stages of cooling and dilution of the ore-forming solutions (Reed, 1982). Silicification of the host rocks involves addition of silica by deposition of quartz and recrystallisation of minerals to a silica-rich assemblage and the rocks produced by the silicification will retain some textural and compositional features of the parent rock. As stated earlier, the silicic rocks of this study are composed mainly of quartz and do not show any replacement features. Further, the alteration products will have similar contents of the generally immobile elements, such as Al, Ti, Zr and P (Cann, 1970; Humphris and Thompson, 1978) as the parent rocks. However, Roberts and Reardon (1978) and Finlow-Bates and Stumfl (1981) noted that intense hydrothermal alteration in the vicinity of the ore deposits may lead to the mobilisation of even these elements. From a detailed study of the petrology of Fennell Formation basalts, Aggarwal (1982) noted that the immobile element compositions of basalts in the Chu Chua area do not show any abnormal patterns of elemental migration, relative to those of the basalts from the barren parts of the Fennell Formation. The much lower Al, Ti, Zr and P contents of the silicic unit compared to the host basalts and their fine-grained nature eliminates the possibility of these rocks being the products of alteration and suggest that they are primary, chemical precipitates i.e. silicic sinters.

Massive talc rocks are also frequently associated with massive sulfide deposits (Franklin *et al.*, 1981). These rocks are generally thought to be produced by the alteration of pyroclastic rocks (Roberts and Reardon, 1978) or ultramafic rocks (Parslow *et al.*, 1981). The talc rocks in the Chu Chua deposit, however, do not show any replacement textures and have very low Al, Ti, Zr and P contents. They are in sharp

contact with the underlying basalts and within one meter of this contact, the chemical and mineralogical composition of these basalts is similar to those from other areas of the deposit. These observations, together with the absence of pyroclastic or ultramafic rocks in the region (Preto, 1979), suggest that the footwall talc rocks in the Chu Chua deposit are also chemical precipitates, i.e. phyllosilicate sinters. Although primary talc precipitates are not known to be associated with massive sulfide deposits, they have recently been reported from the mounds of the hydrothermal vents in the Guaymas Basin, Gulf of California by Lonsdale *et al.* (1980).

C. Environment of Deposition

In order to reconstruct the physical and chemical environment of deposition of the Chu Chua massive sulfides and the footwall rocks, stabilities of talc and minerals in the system Fe – O – S were calculated at 250°C and 300°C as a function of fO_2 and pH (see appendix III). Thermochemical data for minerals and aqueous species given by Helgeson *et al.* (1978) and Helgeson *et al.* (1981) were used in these calculations. Thermodynamic properties of water were taken from Helgeson and Kirkham (1976) and the solubility constants of iron– and copper–chloride complexes were taken from Crerar and Barnes (1976).

Solution Parameters

The solution parameters used in calculating mineral stabilities were chosen on the basis of the composition of fluids in experimental studies of seawater – basalt interaction (Mottl *et al.*, 1978; Seyfried and Bischoff, 1980; Hajash and Archer, 1981), other massive sulfide deposits (Barnes, 1979) and natural hydrothermal systems (Bischoff, 1980). The experimental studies indicate that interaction with basalts enriches the seawater in Si and Fe while depleting it in Mg and that the extent of these elemental exchanges is significantly influenced by the temperature and the water/rock (w/r) ratio. Although there are no independent criteria to estimate this ratio, the solution compositions in many natural hydrothermal systems and volcanogenic massive sulfide deposits, in general, are similar to those observed in experimental studies done at low w/r ratios. Hajash and Archer (1981) noted that seawater reacted with basalts under low w/r ratios (5:1) at 500°C and cooled to 300°C had a silica concentration of 650 ppm

(amorphous silica saturation = 700 ppm). The Mg and Fe concentrations in these solutions were 195 and 222 ppm, respectively. In natural seawater, the Mg concentration is considerably higher (1496 ppm) and that of Fe and Si is much lower (0.1 ppm and 3 ppm respectively). Mixing with seawater would increase the concentration of Mg, and decrease that of Fe and Si, in the upwelling hydrothermal solutions. In the present calculations, an Mg concentration of 10^{-2} moles/ kg water (240 ppm) and Fe concentration of $10^{-2.7}$ moles/ kg water (100 ppm) were assumed. Because the concentration of silica is highly dependent on temperature, saturation with amorphous silica was assumed even though the experimental studies indicate slightly lower concentration. Cu and Cl concentrations of $10^{-3.7}$ moles/kg water (10 ppm) and 1 mol/kg water respectively, were assumed with analogy to generally observed concentrations of these species in ore forming hydrothermal solutions (Barnes, 1979; Arnold and Sheppard, 1981).

Discussion

The stability fields of talc, pyrrhotite, magnetite, pyrite and hematite as a function of fO_2 – pH at 250°C and 300°C are shown in Figures 12 and 13. The relevant reactions and their equilibrium constants are given in appendix III. The calculations were done at the pressure of vapour saturation for water at the given temperature. The activity of FeS in pyrrhotite at 300°C, in equilibrium with pyrite, was estimated from the diagram given by Toulmin and Barton (1964). For pyrrhotite in equilibrium with magnetite, the fugacity of sulfur was approximated by assuming that only one species of sulfur was predominant at a given fO_2 – pH and the activity of FeS was then estimated as above. These values were extrapolated for the calculations at 250°C. The activity of talc was corrected for the Fe–component as

$$activity\ of\ talc = XMg\ /\ XMg + XFe.$$

At 300°C and moderate sulfur concentrations ($10^{-2.5}$ moles), magnetite is stable at a lower fO_2 than pyrite and a stability field of magnetite exists between those of pyrrhotite and pyrite (Fig. 12). At this temperature, talc is stable at a lower pH than iron minerals in the fO_2 region of pyrrhotite stability. Precipitation of talc by the reaction:

$$3\ Mg^{++} + 4\ SiO_2 + 4\ Water = Talc + 6\ H^{+}$$

will buffer the pH of the solution and pyrrhotite would not be stable. With an increase in

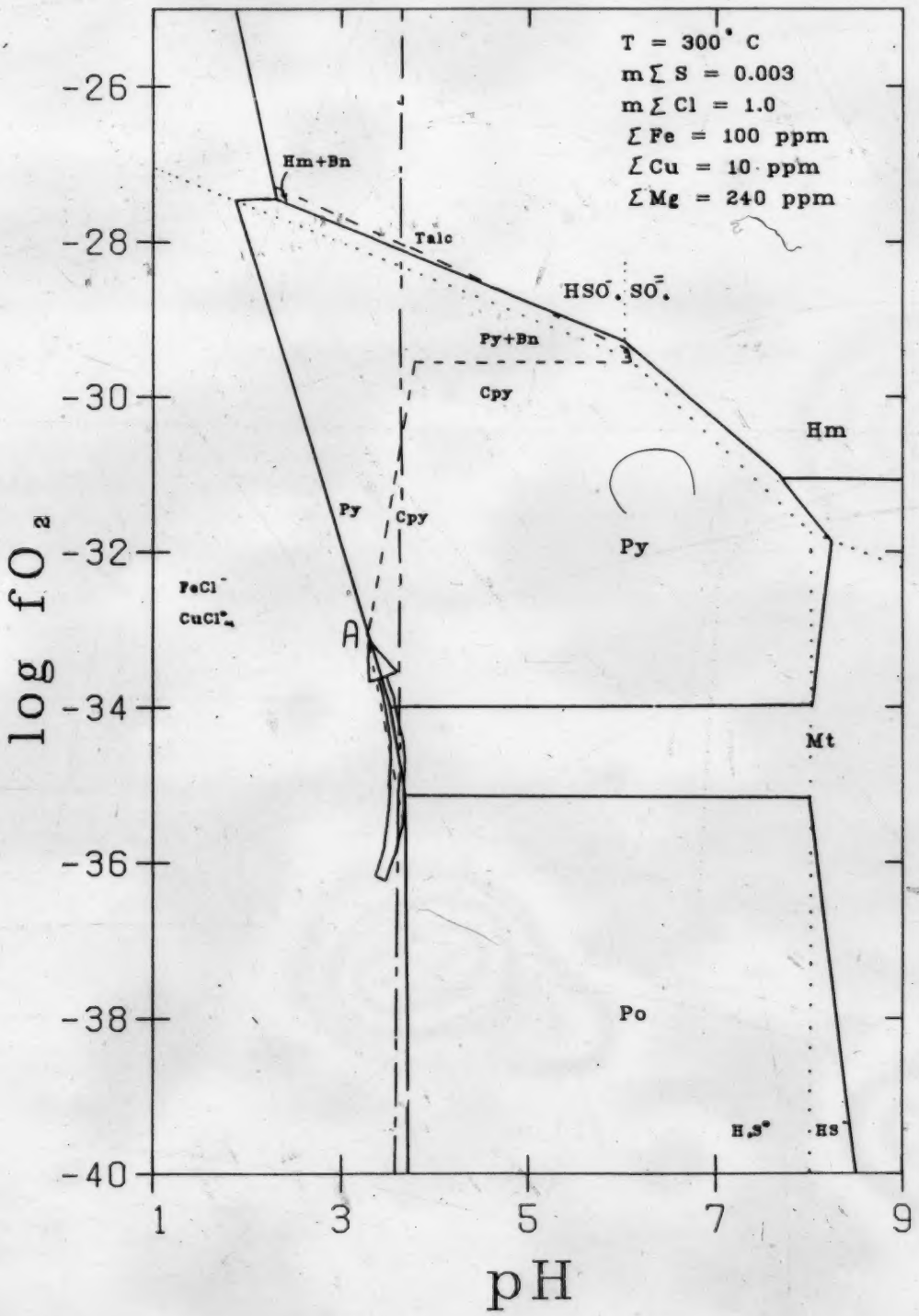

Figure 12. fO_2 – pH diagram at 300°C. Path "A" is as discussed in the text

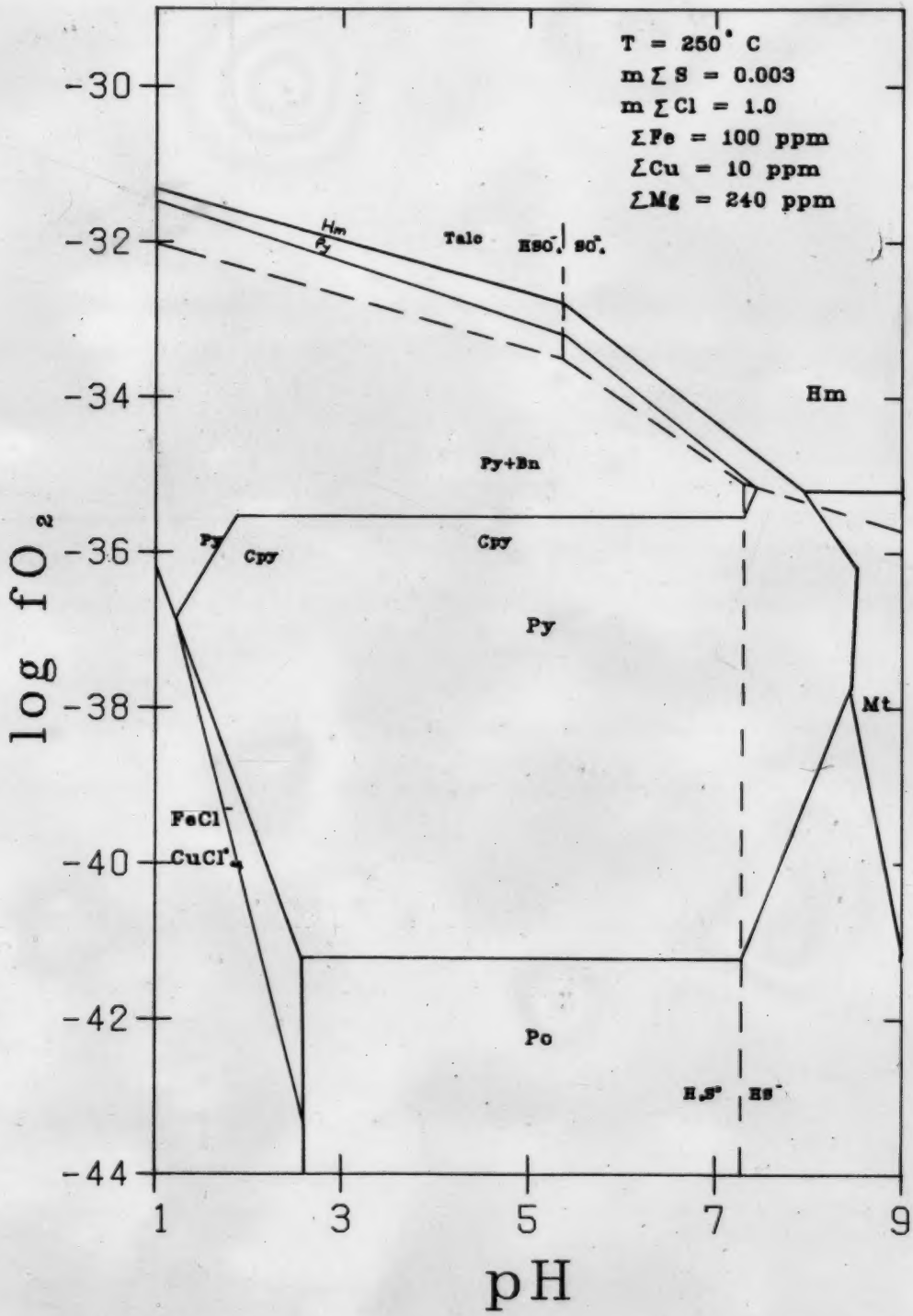

Figure 13. fO_2 – pH diagram at 250°C

fO_2, magnetite would begin to coprecipitate with talc. Under more oxidising conditions, pyrite and chalcopyrite would precipitate and the precipitation of pyrite would buffer the solution pH to more acidic levels than the stability of talc.

Thus, the sequence of precipitation at 300°C, with increasing fO_2, will be:

talc → talc + magnetite → magnetite + pyrite → pyrite + chalcopyrite

This corresponds well with the mineral assemblages observed at the Chu Chua deposit wherein no sulfide minerals occur in the talc body and talc is not present with the sulfides as a gangue mineral. Also, the magnetite content in the talc body increases in the proximity of the sulfides.

At 250°C, the stability fields of talc and magnetite shift significantly. The stability field of magnetite is reduced and in acidic to neutral conditions, magnetite is not stable at a lower fO_2 than pyrite, even with very low (0.001m) sulfur concentrations. Talc is no longer stable at a lower pH than the iron minerals (Fig. 13). The precipitation of pyrite or pyrrhotite buffers the pH to very low levels and talc remains metastable at any oxygen fugacity. Due to the decrease in temperature, the solubility of silica decreases (Walther and Helgeson, 1977) and quartz or amorphous silica may be precipitated (Reed, 1982). With a decrease in temperature and increased mixing of more oxidized seawater, the fO_2 in the hydrothermal solutions also increases. The oxygen fugacity at lower temperatures will be higher than at 300°C and, therefore, above the stability of pyrrhotite. Thus, pyrite, chalcopyrite and silica would be the major minerals precipitating at this temperature. The occurrence of silicic rocks, laterally adjacent to the talc body, is consistent with this observation.

The relative stabilities of minerals discussed above would be significantly different with a change in solution parameters. The stability of talc will shift to more acidic regions at a higher Mg or Si concentration and to alkaline regions at a lower Mg or Si concentration. A higher Fe or S concentration will stabilise pyrrhotite at lower pH than shown in Figures 12 and 13. Thus, given higher Fe and/or S and lower Mg and/or Si concentrations than those assumed in the present calculations, talc may not be stable at a lower pH than iron minerals even at 300°C.

Several lines of evidence support the assumptions of solution parameters made in this study. The occurrence of the silicic sinter unit only laterally adjacent to the massive

talc sinter unit and the absence of silica minerals within the talc unit indicate that during the deposition of talc, the solutions were not super-saturated with respect to silica but became so after cooling. Therefore, the lower limit of Si concentration at 300°C would be at, or close to, amorphous silica saturation as assumed in this study. The Mg concentration is highly dependent on the w/r ratio and the extent of dilution of the hydrothermal solutions on the sea-floor. An increase in both of these factors would result in a higher Mg concentration in the solutions and favor the depostion of talc at lower pH. A Mg concentration of 10^{-2} moles/ kg of water assumed in this study, based upon low w/r ratio and minimal mixing with seawater, can be taken as a lower boundary and higher Mg concentrations will not affect the conclusions reached above. The occurrence of magnetite in and immediately above the talc unit suggests that the solutions were in equilibrium with magnetite in acidic conditions where talc is stable. Solutions with a concentration of sulfur substantially more than 0.003 moles/ kg water can not precipitate magnetite even in slightly alkaline conditions at 300°C (Fig. 12). Consequently, it is reasonable to assume that the maximum concentration of sulfur in the hydrothermal solutions at Chu Chua would have been 0.003 moles/ kg water. The absence of pyrrhotite in the footwall basalts, particularly underneath the talc body, suggests that conditions for its depositon were not reached. Assuming that the molality of sulfur was 0.003, an Fe concentration more than $10^{-3.2}$ moles/kg water (150 ppm) will precipitate pyrrhotite at or below the pH where talc is stable at 300°C (Fig. 12). A decrease in Cu concentration to 1 ppm would shift the pyrite - chalcopyrite boundary to lower fO_2 and chalcopyrite would not coprecipitate with pyrite (Fig. 12). The assumed Fe and Cu molalities of $10^{-3.5}$ (100 ppm) and $10^{-3.7}$ (10 ppm) respectively, therefore, set the upper limit for Fe and lower limit for Cu in the ore solutions at Chu Chua. This is quite realistic in view of the solubility studies of the chalcopyrite + chalcocite and the pyrite + pyrrhotite + magnetite assemblages (Crerer and Barnes, 1976; Crerar *et al.*, 1978). Thus, minor variations in the solution parameters assumed in this study would not significantly change the relative stabilities of the minerals considered.

D. Genetic Model

The stabilities of minerals at the Chu Chua deposit discussed above, suggest that talc was deposited at relatively higher temperatures and lower oxygen fugacities compared to the iron and silica minerals. As seen in Figures 12 and 13, magnetite can coprecipitate with talc only at temperatures higher than 250°C and, therefore, the occurrence of a talc–magnetite lense overlying the talc body is also consistent with this observation.

The relatively higher temperatures and lower oxygen fugacity needed for the deposition of talc in the Chu Chua deposit suggest that the areas of talc sinter deposition represent the exhalative vents of the hydrothermal solutions. This is consistent with the experimental studies on the mixing of hydrothermal solutions with normal seawater (Seyfried and Bischoff, 1980). These authors note that dilution of hydrothermal solutions by small amounts of seawater (mixing ratio 1:3) results in the precipitation of a Mg–phase and, on cooling, of amorphous silica. Also, rapid mixing with large amounts of seawater (mixing ratio 1:39) leads to dilution of silica much below amorphous silica saturation which inhibits the precipitation of magnesian and silica phases. The solutions which deposited talc were probably also responsible for the deposition of the sulfides. Talc, magnetite, and pyrite were deposited close to the vents and in the more distal areas, pyrite and silica were deposited due to lower temperature and more oxidising conditions.

The preceeding discussion suggests that the circulation of seawater due to the extrusion of Fennell Formation basalts and consequent seawater – basalt interaction resulted in the formation of the Chu Chua deposit. This hypothesis can be further evaluated by the lead isotopic compositions of sulfides and the host basalts. The lead isotopic compositions of pyrite and chalcopyrite from Chu Chua are given in Table 6. These compositions are similar to those of basalts from this area (Table 4) as seen in Figure 14. This indicates that the ultimate source of lead in both the sulfides and the host basalts was similar (Thorpe *et al.*, 1981). On this $^{207}Pb/^{204}Pb$ vs $^{206}Pb/^{207}Pb$ diagram (Fig. 14), these compositions give a slope age of 1.56 Ga. However, the geological and other radiometric age determinations of the Fennell Formation (Preto and Schiarriza, 1982) suggest that it is of upper Paleozoic age. It is likely, therefore, that the lead and other metals in the Chu Chua deposit were derived from the basalts or the basement rocks by

Table 6. Lead Isotopic Compositions Of Sulfide Minerals In The Chu Chua Deposit

Sample No.	$^{206}Pb/^{204}Pb$	$^{207}Pb/^{204}Pb$	$^{208}Pb/^{204}Pb$
667	18.52	15.60	38.31
1651	18.48	15.60	38.26
3126A	18.26	15.61	37.32
13106	18.60	15.61	38.32
28129	18.25	15.60	37.87
28141	18.53	15.57	38.06
243	18.57	15.60	38.36
2669	19.09	15.70	38.90
2666	18.86	15.65	38.50
1657	18.53	15.63	38.36
1539	18.68	15.62	38.36
1110	19.03	15.68	39.00
3126B	18.67	15.58	38.19
3139	18.31	15.56	38.02
13137	18.68	15.63	38.51
21204	18.39	15.60	38.23
24272	18.66	15.62	38.37
36179	18.41	15.58	38.16

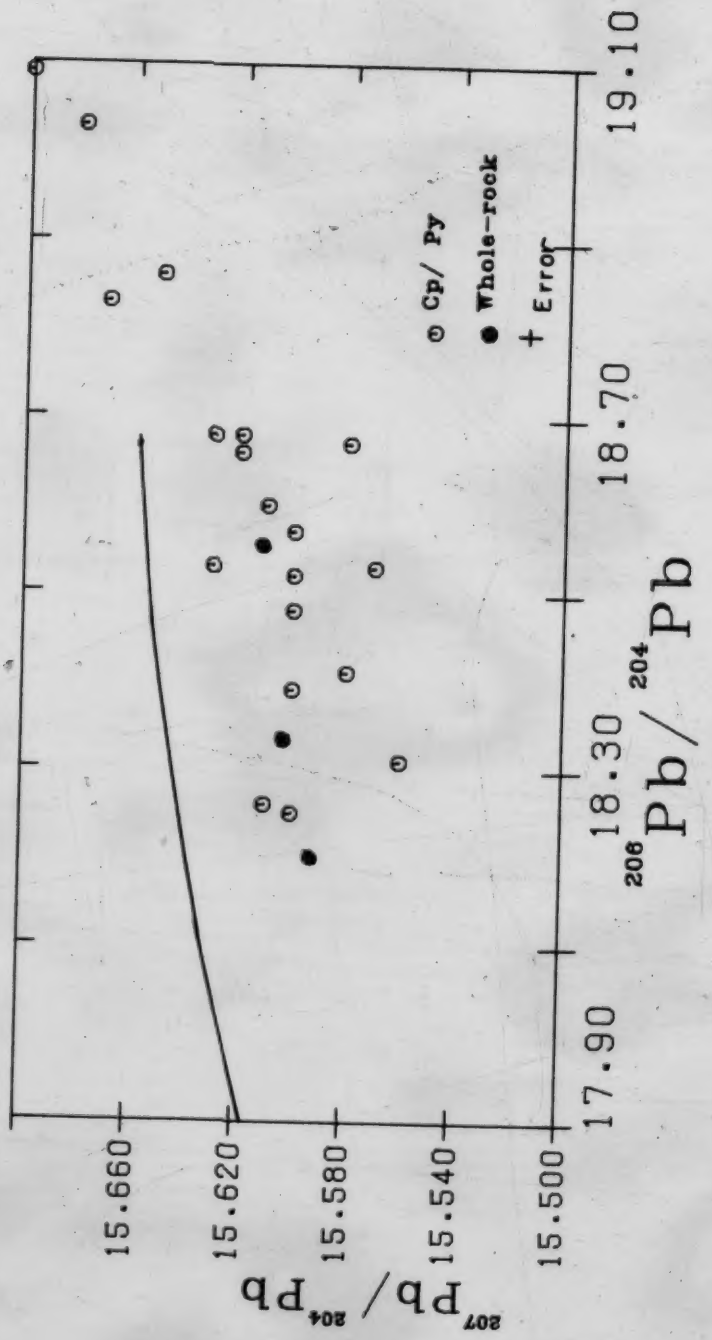

Figure 14. Pb isotopic compositions of pyrite and chalcopyrite from Chu Chua

the circulating seawater (Stacey *et al.*, 1980; Franklin *et al.*, 1981).

The typical footwall metasomatism in volcanogenic massive sulfide deposits, indicated by magnesium enrichment and sodium depletion (Franklin *et al.*, 1981), is not apparent in the host basalts of the Chu Chua deposit (Table 5). There could be two alternative explanations for this observation, namely:

1. The low grade metamorphism in the region may have destroyed the chemically anomalous zones and altered the footwall and the hangingwall basalts to a uniform composition. This seems unlikely, however, in view of the primary alteration zones preserved in massive sulfide deposits which have suffered medium to high grade metamorphism, such as the Anderson Lake and Stall Lake deposits in Manitoba (Franklin *et al.*, 1981).
2. Alternatively, the upwelling solutions did not equilibrate with the rock mass to produce the footwall metasomatism. If the reduced and acidic hydrothermal solutions mix with large amounts of normal seawater before debouching on the sea-floor or rise rapidly through the rock mass without significant cooling, they will not equilibrate with the rocks and will not undergo the elemental exchanges observed in other massive sulfide deposits (Bohlke, 1980). Large-scale dilution of hydrothermal solutions below the rock - water interface is unlikely at the Chu Chua deposit as discussed earlier for the precipitation of talc. The relatively higher temperatures (300°C or more) indicated for talc deposition in the vent areas, however, suggest that the solutions may not have cooled significantly as they ascended towards the rock - water interface. Thus, the apparent lack of footwall metasomatism in the Chu Chua deposit is, most likely, due to a lack of equilibrium interaction between the upwelling solutions and the rock mass.

The presence of trace amounts of tin in the Chu Chua deposit is enigmatic and may also be due to the higher temperatures of deposition. Tin is not commonly associated with massive sulfide deposits and, of the Canadian massive sulfides, economic concentrations of tin are reported from the Sullivan and Kidd Creek deposits. Tin is generally transported as a halide complex and the stability of these complexes is greatly reduced with a decrease in temperature or an increase in pH (Barnes, 1979). Relatively insignificant cooling of the solutions at Chu Chua prior to discharge on the sea-floor

would allow most of the tin to remain in solution and may result in its precipitation with the other sulfide minerals.

The sequence of events in the genesis of the Chu Chua deposit as discussed above is schematically shown in Figure 15. The Fennell Formation basalts were extruded in an ocean island tectonic setting and provided the heat source for the convection of the seawater. The consequent seawater interaction with the basalts resulted in reduced and acidic hydrothermal solutions enriched in Si, Fe, Cu and, probably, reduced sulfur. These solutions rose upwards without much cooling or dilution and did not reequilibrate with the rock mass. The solutions debouched on the sea-floor through at least two vents which varied in their rate and capacity of discharge. The southern vent was probably larger and had a more reducing environment at the sinter mounds as compared to the northern vent. The higher fugacity of oxygen in the southern vent resulted in the depositon of massive talc on the mounds while talc-magnetite were deposited on the northern vent. With an increase in the oxygen fugacity upwards, magnetite and the sulfide minerals were deposited. Laterally distant from the vents, the solutions flowing along the sea-floor cooled and mixed with more oxygenated seawater, depositing sinters composed of silica and the sulfides. The cooling solutions from the larger vent probably covered the sulfides deposited near the smaller vent resulting in the eastern sulfide body being enclosed in the silicic sinter unit. This can be envisioned if the larger vent was deeper and less open than the other, which is consistent with a higher oxygen fugacity at the larger vent.

Applications to exploration for Cu-Fe massive sulfide deposits

Volcanogenic massive sulfide deposits associated with basaltic rocks are generally known to occur in tholeiitic basalts of mid-ocean ridge or island arc tectonic settings (Hutchinson, 1973). The discovery of the Chu Chua deposit in alkalic basalts of an ocean island setting is significant for the exploration for massive sulfide deposits in many basaltic terrains such as the Hawaiian Islands, which have been considered unfavorable so far.

The exploration criteria for ore deposits are aided by prominent geological and geochemical features associated with the ore bodies. In general, the footwall alteration pipe and a stringer zone of sulfides have been useful exploration tools for volcanogenic

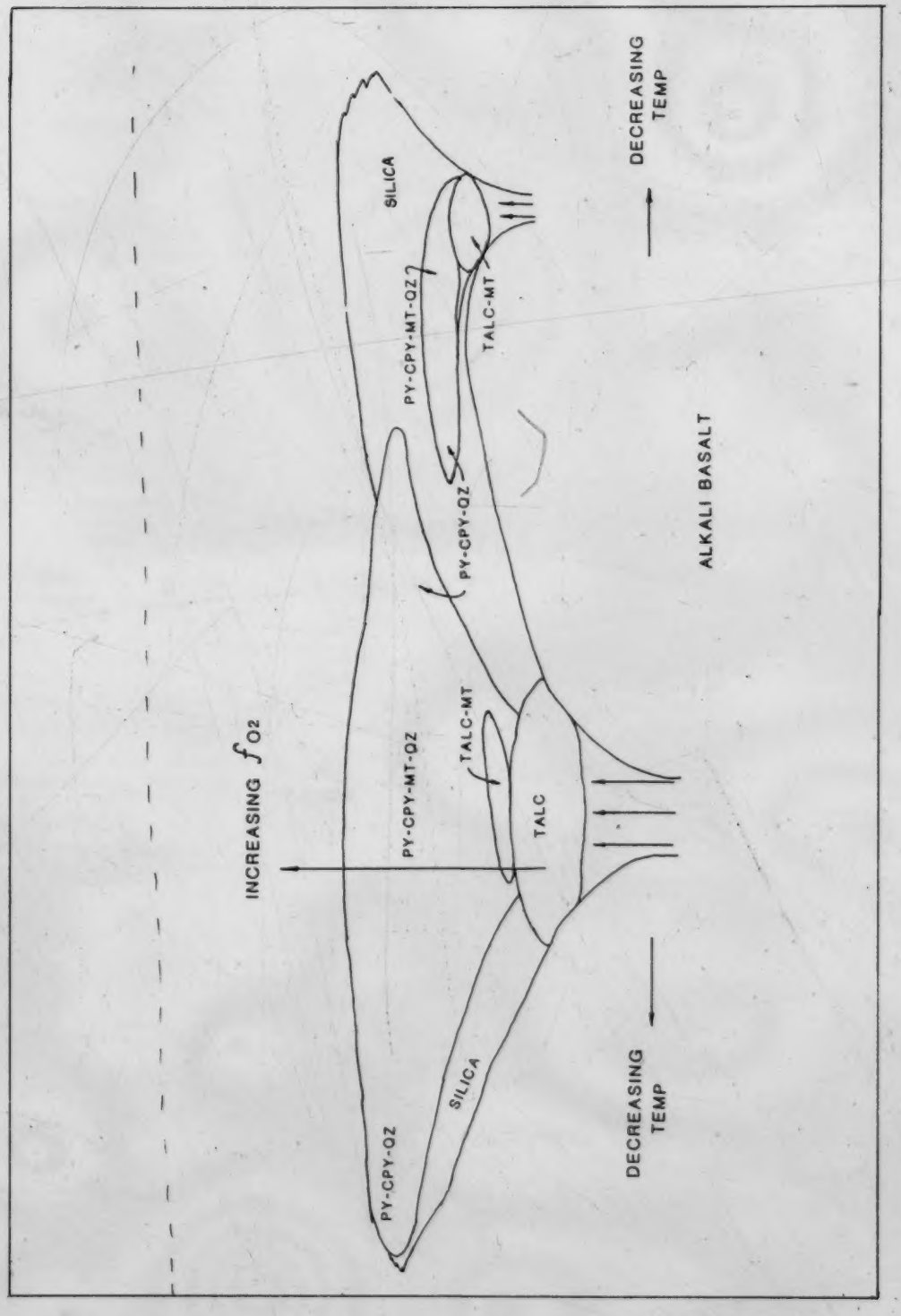

Figure 15. Schematic Sketch for the genesis of the Chu Chua Ore Deposit

massive sulfide deposits (Franklin *et al.*, 1981). Although these zones are not present in the Chu Chua deposit, the associated massive talc and talc–magnetite bodies can be easily identified in the field or geophysical surveys and may be used as a criterion for exploration. In addition, the chemically precipitated silicic rocks are also a likely guide to the ore. Thus, the absence of generally observed footwall alteration zones in a basaltic terrain should not be considered as an indication of the absence of mineralisation. The criteria presented above may provide useful tools in the exploration for massive sulfide deposits, particularly in an ocean island setting.

V. Conclusions

The Chu Chua massive sulfide deposit in south-central British Columbia occurs in the alkalic and transitional basalts of the Fennell Formation which were formed in an ocean island tectonic setting. The deposit consists mainly of two major, stratiform sulfide bodies composed of pyrite and chalcopyrite with minor amounts of sphalerite, cubanite, stannite - kesterite solid solution, magnetite, quartz and calcite. Small lenses of massive talc-magnetite occur partially enclosed in the sulfide bodies. The sulfides are hosted in augite and kaersutite basalts which have been metamorphosed upto low greenschist facies conditions. These basalts have a nearly uniform composition from the footwall to the hangingwall.

Fine-grained, massive silicic and talc rocks occur in the footwall of the sulfide bodies. These rocks do not show any replacement features and have very low Al, Ti, Zr and P contents suggesting that they are primary chemical precipitates. Stabilities of talc and minerals in the system Fe -S - O as a function of fO_2 and pH are consistent with this observation and indicate that the deposition of talc and magnetite is favoured by higher temperatures and lower oxygen fugacity. This suggests that areas of talc deposition represent the vents of the upwelling solutions which were probably also responsible for the depostion of the sulfides. These solutions deposited pyrite and magnetite proximal to the vent area; and pyrite and silica in the distal areas.

The lead isotopic compositions of pyrite and chalcopyrite are very similar to those of the host basalts, indicating a common source of lead. It is suggested that convection of seawater due to the extrusion of the Fennell Formation basalts leached the metals from the basalts or the basement rocks and deposited them on the sea-floor.

VI. References

Aggarwal, PK, 1982, Geochemistry of the Chu Chua massive sulfide deposit: University of Alberta, *unpubl. M.Sc. Thesis.*

Aoki, K, 1963, The kaersutites and oxykaersutites from alkalic rocks of Japan: *J. Petrol.*, 14,p198.

Arnold, M and Sheppard, SMF, 1981, East Pacific Rise at lattitude 21°N: isotopic composition and origin of the hydrothermal sulfur: *Earth Planet. Sci. Letters*, 56, p148-156.

Barnes, HL, 1979, Solubilities of ore minerals *in* HL Barnes (ed) Geochemistry of hydrothermal ore deposits, Wiley, New York, p798.

Barnes, HL and Kullerud, G, 1961,Equilibria in sulfur-containing aqueous solutions, in the system Fe-S-O, and their correlation during ore deposition: *Econ. Geol.*, 56, p 648-688.

Bevins, RE, 1981, Petrology and geochemistry of the Fishguard volcanic complex,Wales: *Geol.Jour.*, 17,p 1-21.

Bischoff, JL, 1980, Geothermal system at 21°N, East Pacific Rise: physical limits on geothermal fluid and role of adiabatic expansion: *Science*, 207, p 1465-1469.

Bischoff, JL and Dickson, FW, 1975, Seawater-basalt interaction at 200° and 500bars: implications for origin of sea floor heavy-metal deposits and regulation of seawater chemistry: *Earth Planet. Sci. Letters*, 25,p385-397.

Bohlke, JK, Honnorez, J and Honnorez-Guerstein, B.-M, 1980, Alteration of basalts from site 396 B, DSDP: petrographic and mineralogic studies: *Contrib. Miner. Petrol.*, 73, p 341-364.

Brandle, JL, 1974, Mineralogy of the materials from Tenegui volcano,La Palma,Canary Islands: *Estud.Geol (Inst.'Lucas Mallada')*, Teneguia volume,p 41-47.

Bryan, WB, 1979, Regional variations and petrogenesis of basalt glasses from the FAMOUS area, Mid-Atlantic ridge: *J.Petrol.*, 20,p293-325.

Campbell, RB and Okulitch, AV, 1973, Stratigraphy and structure of the Mount Ida Group, Vernon, Adams Lake and Bonaparte map areas: *Geol. Surv. Canada*, paper 73-1.

Campbell, RB and Tipper, HW, 1971, Geology of Bonaparte-Lake map area: *Geol. Surv. Can. mem.*,363.

Cann, JE, 1970, Rb, Sr, Y, Zr and Nb in some ocean floor basaltic rocks: *Earth Planet. Sci. Letters*, 10,p7-11.

Carmichael, ISE, Nicholls, J and Smith, AL, 1970, Silica activity in igneous rocks: *Amer.Mineral.*, 55,p246-263.

Carmichael, ISE,Turner, FJ and Verhoogen, J, 1974,Igneous Petrology: McGraw Hill, New York, p 739.

Cathles, LM, 1981, Fluid flow and genesis of hydrothermal ore deposits: *Econ.Geol.*, 75th anniversary vol., p424-457.

Cawthorn, FG, 1976a, Amphibole stability and liquid evolution trends in hydrous synthetic basaltic compositions at 5kb: *Progr.Exptl.Petrol., NERC publ.London*, seriesD, 6, p274-275.

Cawthorn, FG, 1976b, Some chemical controls on the composition of igneous amphiboles: *Geochim. Cosmochim. Acta*, 39,p22-33.

Chayes, F, 1964, A petrological distinction between Cenozoic volcanics in and around the open oceans: *Jour.Geophys.Res.*, 69, p1573-1588.

Crerar, DA and Barnes, HL, 1976, Ore solution chemistry V: solubility of chalcocite and chalcopyrite assemblages in hydrothermal solutions at 200°C and 350°C: *Econ. Geol.*, 71, p 772-794.

Crerar, DA, Susak, NJ, Borcsik, M and Schwartz, S, 1978, Solubility of the buffer assemblage pyrite + pyrrhotite + magnetite from 200°C to 350°C: *Geochim. Cosmochim. Acta*, 42, p 1427-1437.

Dick, HJB, 1982, The petrology of two back-arc basins of the northern Phillipine sea: *Amer. J. Sci.*,282,p644-700.

Floyd, PA and Winchester, JA, 1975, Magma type and tectonic setting discrimination using immobile elements: *Earth Planet. Sci. Letters*, 27,p211-218.

Finlow-Bates, T and Stumfl, EF, 1981,The behaviour of so-called immobile elements in te hydrothermally altered rocks associated wit volcanogenic submarine-exhalative ore deposits: *Mineral Deposita*, 16, p 319-328.

Franklin, JM, Sangster, DF and Lydon, JW, 1981, Volcanoic - associated massive sulfide deposits: *Econ.Geol.*, 75th anniversary vol., p 485-627.

Fodor, RV, Keil,K and Bunch,TE, 1975, Contributions to the mineral chemistry of Hawaiian rocks IV: pyroxene compositions in rocks from Haleakala and West Maui volcanoes, Maui,Hawaii: *Contrib. Miner. Petrol.*,50,p173-195.

Gast, PW, 1968, Trace element fractionation and the origin of tholeiitic and alkaline magma types: *Geochim. Cosmochim. Acta*,32,p1057.

Grenne, J and Roberts, D, 1980, Geochemistry and volcanic setting of the ordovician Forbordfjell and Jonsvatn greenstones, Trondheim region, Central Norwegian Caledonides: *Contrib. Miner. Petrol.*, 74, p 375-386.

Gunn, BM, 1972, The fractionation effect of kaersutite in basaltic magmas: *Can.Miner.*, 11, p 840-850.

Gupta, AK,Onuma, K,Yagi, K and Lidiak, EG,1973, Effect of silica concentration on the diopsidic pyroxenes in the system diopside-$CaTiAl_2O_6$-SiO_2: *Contrib. Miner. Petrol.*, 41,p333-344.

Hajash, A,1975, Hydrothermal processes along mid-ocean ridges, an experimental study: *Contrib. Miner. Petrol.*, 53,p205-226.

Hajash, A and Archer, P,1981, Experimental sea water basalt interaction: effects of cooling: *Contrib. Miner. Petrol.*, 75,p1-13.

Hajash, A and Chandler, GW,1981, An experimental investigation of high temperature interactions between seawater and rhyolite, andesite, basalt and peridotite: *Contrib. Miner. Petrol.*, 78,p240-254.

Hall-Bayer, B,1976, Geochemistry of some ocean-floor basalts British Columbia: University of Alberta, *unpubl.M.Sc.Thesis*,p 105.

Hart, R,1970, Chemical exchange between sea water and deep ocean basalts: *Earth Planet. Sci. Letters*, 19,p269-279.

Hart, SR,1969, K, Rb, Cs contents and K/Rb, K/Cs ratios of fresh and altered submarine

basalts: *Earth Planet. Sci. Letters*, 6,p295-303.

Hart, SR, Erlank, AJ and Kable, EJD, 1974, Seafloor basalt alteration: some chemical and strontium isotopic effects: *Contrib. Miner. Petrol.*, 44,p219-230.

Helgeson, HC and Kirkham, DH, 1974, Theoretical prediction of the thermodynamic behaviour of aqueous electrolytes at high pressures and temperatures:I. summary of the thermodynamic / electrostatic properties of the solvent: *Amer. J. Sci.*, 274, p 1089-1198.

Helgeson, HC, Kirkham, DH and Flowers, GC, 1981, Theoretical prediction of the thermodynamic behaviour of aqueous electrolytes at high pressures and temperatures:IV. calculation of activity coefficients, osmotic coefficient and apparent molal properties to 600°C and 5 Kb: *Amer. J. Sci.*, 281, p 1249-1516.

Helgeson, HC, Delany, JM, Nesbitt, HW and Bird, DK, 1978, Summary and critique of the thermodynamic properties of rock forming minerals: *Amer. J. Sci.*, 278A, p229.

Holm, P, 1982, Non-recognition of continental tholeiites using the Ti-Zr-Y diagram: *Contrib. Miner. Petrol.*, 79, p 308-310.

Humphris, SE and Thompson, G, 1978a, Hydrothermal alteration of oceanic basalts by sea water: *Geochim. Cosmochim. Acta*, 42, p107-126.

Humphris, SE and Thompson, G, 1978b, Trace element mobility during hydrothermal alteration of oceanic basalts: *Geochim. Cosmochim. Acta*, 42,p127-136.

Hutchinson, RW, 1973, Volcanogenic sulfide deposits and their metallogenic significance: *Econ. Geol.*, 68, p 1223-1246.

Hynes, A, 1980, Carbonatization and mobility of Ti, Y and Zr in ascot formation metabasalts, SE Quebec: *Contrib. Miner. Petrol.*, 75, p 79-87.

Kesson, S and Price, RC, 1972, The major and trace element chemistry of kaersutite and its bearing on the petrogenesis of alkaline rocks: *Contrib. Miner. Petrol.*, 35, p 119-124.

Krstic, D, 1981, Geochronology of the Charlebois Lake area, northeastern Saskatchewan: University of Alberta, *unpublished M.Sc. thesis*, 1981, p 89.

Kushiro, I, 1960, Si-Al relations in clinopyroxenes from igneous rocks: *Amer. J. Sci.*, 258,p548-554.

Kushiro, I, 1972, Determination of liquidus relations in synthetic silicate systems with electron probe analysis: the system forsterite - diopside - silica at 1 atmosphere: *Amer.Mineral.*, 57,p1260-1271.

LeBas, MJ, 1962, The role of aluminum in igneous clinopyroxenes with relation to their parentage: *Amer. J. Sci.*, 260,p267-288.

Leake, BE, 1978, Nomenclature of amphiboles: *Amer. Miner.*, 63, p 1023-1052.

Leterrier, J, Maury, RL, Thoron, P, Girard, D and Marchal, M, 1982, Clinopyroxene composition as a discriminant for the identification of the magmatic affinities of paleo-volcanic series: *Earth Planet. Sci. Letters*, 59, p139-154.

Longstaffe, FJ, 1978, Oxygen isotope and elemental geochemistry of Archean silicate rocks from northern Ontario: McMaster University, *unpublished Ph.D. thesis*, p546.

Lonsdale, PF, Bischoff, JL, Burns, VM, Kastner, M and Sweeney, RE, 1980, A high-temperature hydrothermal deposit on the seabed at a gulf of California spreading centre: *Earth Planet. Sci. Letters*, 49, p 8-20.

McMillan, WC, 1980, Geology of the Chu Chua massive sulfide deposit, south-central British Columbia: *abstr., Geol. Assoc. Can.*, cordilleran section, ann.mtg., p 20.

McBirney, AR and Gass, IG, 1967, Relations of oceanic volcanic rocks to mid-ocean rises and heat flow: *Earth Planet. Sci. Letters*, 2,p265-276.

McDonald, GA and Katsura, T, 1964, Chemical composition of Hawaiian lavas: *J.Petrol.*, 5,p82-133.

Melson, WG and Thompson, G, 1971, Petrology of a transform fault and adjacent ridge segments: *R. Soc. London phil. trans.*, A-26,p423-441.

Miyashiro, A, Shido, F and Ewing, M, 1969, Diversity and origin of of abyssal tholeiite from the Mid-Atlantic ridge near 24° and 30° north lattitude: *Contrib. Miner. Petrol.*, 23,p38-52.

Monger, JWH, 1977, Upper Paleozoic rocks of the Western Canadian Cordillera and their bearing on Cordilleran evolution: *Can. J. Earth Sci.*, 14,p1832-1859.

Mottl, MJ and Holland, HD, 1978, Chemical exchange during hydrothermal alteration of basalts by seawater I. experimental results for major and minor components of seawater: *Geochim. Cosmochim. Acta*, 42,p1103-1115.

Nisbet, EG and Pearce, JA, 1977, Clinopyroxene composition in mafic lavas from different teconic settings: *Contrib. Miner. Petrol.*, 63,p149-160.

Papike, JJ, Cameron, KL and Baldwin, K, 1974, Amphiboles and Pyroxenes:characterisation of other than quadrilateral components and estimation of ferric iron from microprobe data: *Geol.Soc.Amer., abstr. with program*, p1054-1055.

Parslow, GR, Watters, BR and McDougall, FH, 1981, Chemistry and origin of carbonate-rich rocks in the area of Amisk Lake (East), Saskatchewan: *CIM Bull.*, 74, p81-86.

Pearce, JA and Cann, JR, 1973,Tectonic setting of basic volcanic rocks determined using trace element analyses: *Earth Planet. Sci. Letters*, 19,p290-300.

Preto, VA, 1979, Barrier Lakes-Adams Plateau area: *B.C.dept.ener.mines res.*, paper 1979-1c, p31-37.

Preto, VA and Schiarriza, P. 1982, Geology and mineral deposits of the Eagle-Bay and Fennell Formation from Adams plateau and Clearwater,south-central B.C.: *Geol.Assoc.Canada, Cordilleran section, abstr with progr.*, p22-24.

Reed, MH, 1982, Calculation of multicomponent chemical equilibria and reaction processes in systems involving minerals, gases and an aqueous phase: *Geochim. Cosmochim. Acta*, 46, p 513-528.

Roberts, RG and Reardon, EJ, 1978, Alteration and ore-forming processes at mattagami lake mine, Quebec: *Can. J. Earth Sci.*, 15, p 1-21.

Sack, RO,Carmichael, ISE,Rivers, M and Ghiorso, MS, 1980, Ferric-ferrous equilibria in natural silicate liquids at 1bar: *Contrib. Miner. Petrol.*, 75,p369-376.

Scarfe, CM and Smith, DGW, 1977, Secondary minerals in some basaltic rocks from DSDP Leg 37: Can. J. Earth Sci., 14, p 903-910.

Schweitzer, EL, Papike, JJ and Bence, AE, 1979, Statistical analysis of clinopyroxene from deep-sea basalts: *Amer. Miner.*, 64, p 501-513.

Seyfried, W and Bishcoff, J, 1980, Hydrothermal transport of heavy metals by seawater: the role of seawater/basalt ratio: *Earth Planet. Sci. Letters*, 34, p 71-77.

Smith, D and Lindsley, DH, 1971, Stable and metastable augite crystallisation trends in a single basalt flow: *Amer.Mineral.*,56,p225,233.

Smith, DGW and Gold, CM, 1979, EDATA2: a Fortran IV computer program for processing wavelength and/or energy-dispersive electron microprobe data: *Proc. 14th Ann. Conf. Microbeam Anal. Soc.*, San Antonio, Texas, p 273-278.

Stacey, JS, Doe, BR, Roberts, RJ, Delevaux, MA and Granlich, JW, 1980, A lead isotopic study of mineralization in the Saudi Arabian shield:*Contrib. Miner. Petrol.*, 74, p175-188.

Tatsumoto, M, 1978, Isotopic composition of lead in oceanic basalts and its implication to mantle evolution: *Earth Planet. Sci. Letters*,38,p63-87.

Thorpe, RI, Franklin, JM and Sangster, DF, 1981, Evolution of lead in massive sulphide ores of Bathurst district, New Brunswick, Canada: *Inst. Mining Met. Trans.*, 90, p B55-B56.

Toulmin, P and Barton, PB, 1964, A thermodynamic study of pyrite and pyrrhotite: *Geochim. Cosmochim. Acta*, 28, p 641-671.

Sun, SS,1980, Lead isotopic study young volcanic rocks from mid-ocean ridges, ocean islands and island arcs: *R. Soc. London phil. trans.*, A 297, p409-445,

Vollo, N, 1981, Geology and regional setting of the Chu Chua copper deposit, southcentral British Columbia: *Can. Instt. Min. Metal.*, 74, p60.

Walther, JV and Helgeson, HC, 1977, Calculation of the thermodynamic properties of aqueous silica and the solubility of quartz and its polymorphs at high pressure and temperature: *Amer. J. Sci.*, 277, p1315-1351

Wilkinson, JGF,1961, Some aspects of the calciferrous amphiboles, oxyhornblendes, kaersutite and Barkevikite: *Amer. Miner.*, 46, p340-354.

Wilkinson, JGF,1982, The genesis of mid-ocean ridge basalt: *Earth-Sci. Rev.*, 19, p1-57.

Winkler, HGF, 1979, Petrogenesis of metamorphic rocks, 5th ed., Springer, Berlin, p 290.

Wood, DA,Joron, J and Treuil, M,1979, A reappraisal of the use of trace elements to classify and discriminate between magma series erupted in different tectonic settings: *Earth Planet. Sci. Letters*, 45, p326-336.

VII. Appendix I: Sample Locations And Mineral Assemblages

Samples for this study were collected from drill core of forty two holes drilled in the vicinity of the Chu Chua deposit. The surface locations of the holes are shown in Figure Ia. Mineral assemblages observed in polished-thin sections are given in Table Ia.

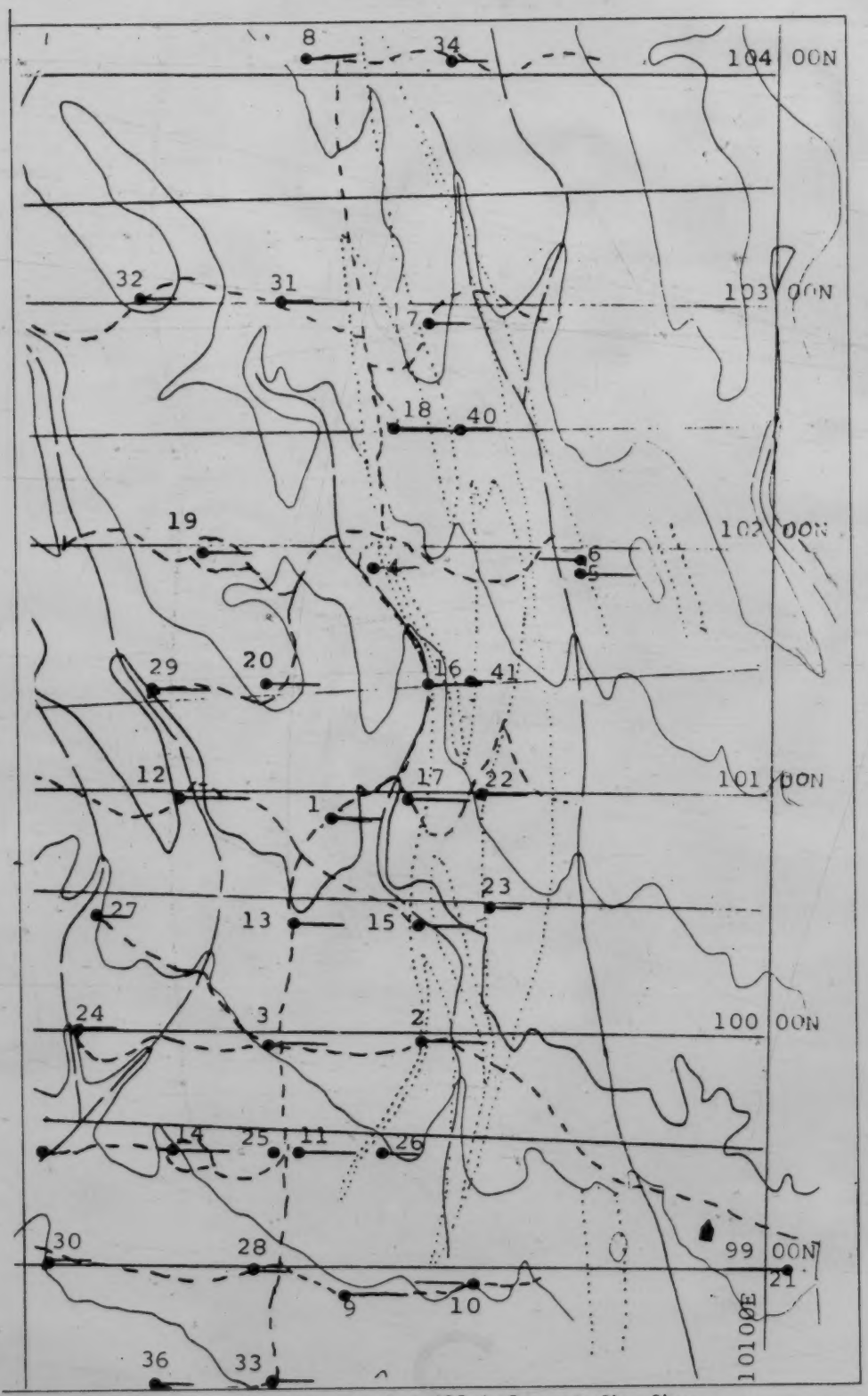

Figure 1a. Surface locations of drill holes at Chu Chua.

Table Ia. Mineral Assemblages Observed In Thin Sections

No.	RT	Cpx	Kar	Plg	Ilm	Act	Chl	Zo	Sph	Mt	Qz	Py	Phe	Tc	Cb
110	1	X		X		X	X	X	X	X					X
129	2	X		X		X	X	X	X	X					X
190	3									X				X	X
191	3			X		X	X	X	X		X	X			
1101	1						X				X		X		
1116	2						X				X		X		
1128	1	X		X		X	X	X	X	X					X
3144	2						X				X	X	X		X
3134	2						X		X		X	X	X		X
448	2						X				X		X		
4113	1	X		X	X	X	X	X	X	X		X			X
4183	1	X		X	X	X	X	X	X	X		X			X
4196	1	X		X	X	X	X	X	X	X					X
4206	1	X		X	X	X	X	X	X	X					X
516	1	X		X	X	X	X	X	X	X					X
581	1	X		X	X	X	X	X	X	X				?	X
582	1	X		X	X	X	X	X	X	X				?	X
628	2						X				X		X		X
670	2						X			X	X		X		X
714	1						X				X	X	X		
729	2						X				X	X	X		
742	2			X	X	X	X	X	X	X					X
13113	2						X				X	X	X		X
13120	2						X				X		X		X
13139	2						X				X	X	X		X
13141	2						X				X		X		X
1565	2						X				X		X		X
1569	2						X				X		X		X
1575	2						X			X	X		X		X
1577	2						X				X		X		X
1580	1						X				X		X		X
1581	1			X	X	X	X	X	X	X	X				X
1590	1	X		X	X	X	X	X	X	X	X				X
1596	1			X	X	X	X	X	X	X	X				X
1666	2						X				X		X		X

No.	RT	Cpx	Kar	Plg	Ilm	Act	Chl	Zo	Sph	Mt	Qz	Py	Phe	Tc	Cb
1670	1	X		X	X	X	X	X	X						X
1680	1	X		X	X	X	X	X	X		X				X
1774	1	X		X	X	X	X	X	X						X
1784	1	X		X	X	X	X	X	X		X				X
1799	1	X		X	X	X	X	X	X						X
17100	1	X		X	X	X	X	X	X						X
1817	2						X				X	X	X		
1828	1			X	X	X	X	X	X		X				X
1841	2						X		X		X		X		X
1849	1						X		X		X		X		X
1893	1	X	X	X	X	X	X	X	X						
1896	1	X		X	X	X	X	X	X						X
18104	1	X		X	X	X	X	X	X						X
20107	2						X				X		X		X
20110	2						X				X		X		X
2129	1	X		X	X	X	X	X	X		X				
2164	1	X		X	X	X	X	X	X	X					
21109	1	X		X	X	X	X	X	X	X					
21193	1	X		X	X	X	X	X	X	X					
21202	1	X		X	X	X	X	X	X	X					
21224	1	X		X	X	X	X	X	X	X					
2244	2						X				X		X		X
2254	1	X	X	X	X	X	X	X	X						X
2485	1	X		X	X	X	X	X	X	X					
24263	1	X		X	X	X	X	X	X		X				X
24269	1	X		X	X	X	X	X	X						X
24273	1			X	X	X	X	X	X		X				X
24303	1			X	X	X	X	X	X		X				X
2551	1	X		X	X	X	X	X	X		X				X
2556	3						X		X					X	X
25100	2									X				X	
25101	2									X				X	
25140	2					X				X				X	
25141	2					X				X				X	
25159	1	X		X	X	X	X	X	X		X				X
2644	3									X				X	
2654	3									X				X	
2670	3					X				X				X	X

No.	RT	Cpx	Kar	Plg	Ilm	Act	Chl	Zo	Sph	Mt	Qz	Py	Phe	Tc	Cb
2715	1	X	X	X	X	X	X	X	X	X					
27237	2										X				X
27257	1					X	X	X			X				X
27253	1			X	X									?	X
27261	1	X	X	X	X	X	X	X	X		X				X
2874	1	X	X	X	X	X	X	X	X						X
28146	1		X	X		X	X	X	X	X	X				X
28149	1	X		X	X	X	X	X	X						X
30107	1	X		X	X	X	X	X	X		X				
30154	1	X		X	X	X	X	X	X						
30241	1	X		X	X	X	X	X	X						
30271	1			X	X	X	X	X							X
3286	1	X		X	X	X	X	X	X						
32156	2						X				X		X		
3413	1	X	X	X	X	X	X	X	X						
3420	1										X				X
3449	1			X	X	X	X	X	X		X				X
3452	1			X	X	X	X	X	X		X				X
3458	1	X	X	X	X	X	X	X	X	X					X
3459	1	X		X	X	X	X	X	X	X					X
3463	1	X		X	X	X	X	X	X						X
3466a	1		X	X	X	X	X	X	X						
3466b	1	X	X	X	X	X	X	X	X						
3514	2										X		X		X
3562	2						X				X		X		X
3599	1			X		X	X		X		X				X
35108	1			X		X	X		X		X	X			X
3648	1	X		X	X		X		X						X
36179	1			X	X	X	X	X	X						X
36182	1	X		X	X	X	X	X	X						X
36194	1	X	X	X	X	X	X	X	X						X
36199	1	X		X	X	X	X	X	X						X
3725	1					X	X	X			X				X
36199	1			X	X	X	X	X	X		X				X
3742	2						X				X	X	X		X
3770	2						X				X	X	X		X
37139	1	X		X	X	X	X	X	X						X
37142	1	X		X	X	X	X	X	X						

No.	RT	Cpx	Kar	Plg	Ilm	Act	Chl	Zo	Sph	Mt	Qz	Py	Phe	Tc	Cb
3893	1	X		X	X	X	X	X	X						X
38280	1	X		X	X	X	X	X	X						
3915	1	X		X	X	X	X	X	X						X
3947	2						X				X		X		X
3962	1	X		X	X	X	X	X	X		X				X
3964	1	X		X	X	X	X	X	X		X				X
3980	1	X		X	X	X	X	X	X						X
3992	1	X		X	X	X	X	X	X						X
39125	1	X		X	X	X	X	X	X						X
39149	2						X				X	X	X		X
4027	2						X				X		X		X
4037	2							X			X				X
4115	1			X				X	X		X				X

RT	Rock Type (1=Basalt, 2=Silicic unit, 3=Talc unit)
Cpx	Clinopyroxene – Augite
Plg	Albitised plagioclase
Kar	Kaersutite
Ilm	Altered Fe-Ti Oxides
Act	Actinolite
Chl	Chlorite
Zo	Zoisite
Sph	Sphene-leucoxene
Mt	Magnetite
Qz	Quartz
Py	Pyrite
Phe	Phengite
Tc	Talc
Cb	Carbonate

VIII. Appendix II: Chemical Analyses

Twenty two samples of basalts, thirty pyroxene grains and eighteen amphibole grains were analysed for their chemical composition. Representative analyses are given in the main text and complete sets of analyses are given in this appendix, Tables IIa – IIc.

Table IIa. Whole-Rock Analyses[1] of Basaltic Rocks From Chu Chua

No.	SiO_2	Al_2O_3	Fe_2O_3	MgO	CaO	Na_2O	K_2O	TiO_2	MnO	P_2O_5	Zr
1700	49.49	15.21	11.84	7.92	10.39	3.07	0.06	1.62	0.19	0.20	123
110	50.68	14.27	11.43	7.31	9.90	4.20	0.05	1.76	0.18	0.21	130
2846	53.35	15.49	11.45	9.07	5.84	0.23	2.19	2.00	0.17	0.20	121
1680	62.17	12.53	8.42	5.00	5.87	4.11	0.06	1.45	0.18	0.21	154
2559	49.07	15.77	10.68	6.45	13.94	1.87	0.04	1.77	0.18	0.23	126
2551	50.58	14.44	12.24	7.48	10.25	2.71	0.08	1.78	0.22	0.22	119
1581	50.21	14.60	13.85	8.76	8.09	2.02	0.07	1.89	0.31	0.20	123
548	53.49	13.38	8.02	5.84	17.59	0.15	0.04	1.20	0.12	0.17	93
3925	50.96	14.57	13.40	8.38	6.85	3.11	0.07	2.06	0.37	0.22	140
1893	50.46	14.48	11.63	7.05	10.13	3.92	0.04	1.88	0.19	0.21	132
3459	47.61	14.13	14.99	8.96	9.61	2.04	0.04	2.18	0.23	0.20	123
3893	49.78	14.85	11.64	7.39	11.49	2.34	0.29	1.83	0.18	0.21	130
2473	44.86	14.86	14.00	9.61	9.46	4.15	0.72	1.90	0.24	0.19	114
2485	50.71	14.59	11.63	6.71	11.82	2.06	0.31	1.78	0.19	0.21	129
2715	50.10	15.79	11.94	6.81	10.13	2.69	0.22	1.9	0.19	0.22	129
3413	54.44	14.70	11.34	5.74	7.30	3.99	0.04	1.99	0.23	0.24	160
3458	54.50	15.13	10.85	5.36	8.16	3.68	0.04	1.9	0.19	0.19	130
3694	50.50	15.45	11.29	7.43	10.61	2.01	0.69	1.66	0.17	0.18	119
581	40.40	18.89	14.46	11.19	9.56	1.12	1.73	2.19	0.19	0.28	154
582	52.69	14.31	11.50	7.88	8.02	1.44	1.75	2.04	0.18	0.18	122
1596	51.11	16.44	10.39	7.01	10.88	2.09	0.19	1.54	0.17	0.17	115
3742	50.97	16.52	9.65	7.34	11.23	2.38	0.33	1.26	0.17	0.14	98

[1] recalculated on a volatile free basis

Table IIb. Pyroxene Analyses[1]

No.	4592	4962	1392	2241	2242	2151	7152	7153	8932	1941	1991	7841	7845	9151	9154
SiO_2	49.55	48.27	50.57	51.20	49.44	48.62	47.66	48.14	46.04	48.07	51.62	47.20	50.99	50.22	52.54
Al_2O_3	5.18	5.54	6.37	3.51	4.25	5.71	5.92	5.83	8.10	5.42	2.48	4.09	4.51	2.27	2.25
TiO_2	1.25	1.44	0.44	0.99	1.28	1.68	2.09	1.85	2.55	1.82	0.68	0.76	0.92	0.50	0.60
FeO	7.27	7.14	7.19	8.76	9.36	9.05	8.98	9.34	9.52	9.93	8.52	6.31	6.60	6.54	7.43
Fe_2O_3	0.87	1.22	0.0	0.0	0.0	0.0	0.0	0.13	0.0	0.06	0.0	0.0	0.0	0.0	0.0
MgO	14.47	13.97	13.76	15.83	14.47	14.04	13.42	13.64	11.85	13.17	17.08	16.40	16.22	18.39	15.78
CaO	21.20	20.97	21.19	19.15	19.41	19.73	20.15	19.83	20.52	19.91	17.74	19.43	19.16	17.91	19.27
Cr_2O_3	0.32	0.21	0.19	0.23	0.13	0.18	0.14	0.15	0.16	0.17	0.20	0.37	0.40	0.45	1.08
MnO	0.16	0.13	0.16	0.18	0.18	0.14	0.15	0.18	0.17	0.21	0.21	0.14	0.10	0.19	0.18
Na_2O	bdl	bdl	bdl	bdl	bdl	bdl	bdl	bdl	bdl	bdl	bdl	bdl	bdl	bdl	bdl
Total	100.1	98.76	99.87	99.35	98.51	99.16	98.51	99.08	98.77	98.76	98.53	98.39	98.83	97.85	97.42

No. Of Cations On The Basis Of 6 Oxygens

Si	1.84	1.83	1.87	1.90	1.87	1.83	1.81	1.82	1.75	1.82	1.93	1.89	1.88	1.94	1.92
Al	0.23	0.25	0.28	0.15	0.19	0.25	0.26	0.26	0.36	0.24	0.11	0.18	0.20	0.10	0.10
Ti	0.03	0.04	0.01	0.03	0.04	0.05	0.06	0.05	0.07	0.05	0.02	0.02	0.03	0.01	0.02
Fe^{2+}	0.23	0.23	0.22	0.27	0.30	0.28	0.28	0.29	0.30	0.32	0.27	0.20	0.21	0.20	0.24
Fe^{3+}	0.02	0.03	0.0	0.0	0.0	0.0	0.0	0.00	0.0	0.00	0.0	0.0	0.0	0.0	0.0
Mg	0.80	0.79	0.76	0.87	0.81	0.79	0.76	0.77	0.67	0.74	0.95	0.91	0.90	1.01	0.89
Ca	0.84	0.85	0.84	0.76	0.79	0.79	0.82	0.80	0.83	0.81	0.71	0.77	0.77	0.71	0.79
Cr	0.01	0.01	0.01	0.01	0.00	0.01	0.00	0.00	0.00	0.01	0.01	0.01	0.01	0.01	0.03
Mn	0.01	0.00	0.00	0.01	0.01	0.00	0.00	0.01	0.01	0.01	0.01	0.00	0.00	0.01	0.01
Wo	45.11	45.61	46.12	39.88	41.44	42.59	43.97	43.02	46.18	43.31	36.84	41.20	40.88	36.86	40.98
FS	12.07	12.12	12.22	14.25	15.60	15.25	15.29	15.82	16.72	16.86	13.81	10.44	10.99	10.50	12.33
En	42.81	42.27	41.66	45.86	42.96	42.16	40.74	41.17	37.10	39.84	49.34	39.52	48.36	48.13	52.64

Table IIb (contd.)

No.	3459	4196	3739	1784	7842	7843	2715	7154	3699	6199	1993	1996	6997
SiO_2	49.90	49.48	51.85	50.98	51.39	51.15	52.04	52.01	49.58	50.84	48.39	49.93	49.29
Al_2O	4.82	5.14	3.03	4.10	4.20	4.61	2.39	2.32	4.58	4.08	4.55	4.74	4.87
TiO_2	1.15	1.37	0.72	0.76	0.92	0.95	0.63	0.63	1.66	1.18	2.05	1.41	1.58
FeO	7.30	6.99	8.06	6.33	7.70	6.74	7.81	7.67	9.94	8.42	13.68	9.32	10.45
Fe_2O_3	0.62	0.83	0.0	0.0	0.0	0.0	0.0	0.0	0.0	0.0	0.28	0.0	0.24
MgO	14.50	14.63	15.95	16.39	16.25	16.51	16.04	16.24	14.32	15.13	13.13	14.55	14.26
CaO	21.41	21.26	19.95	19.43	19.18	19.51	20.10	19.83	19.48	19.97	17.36	19.61	18.98
Cr_2O_3	0.24	0.29	0.23	0.36	0.19	0.41	0.81	1.11	0.23	0.22	0.18	0.22	0.18
MnO	0.13	0.10	0.22	0.14	0.15	0.10	0.19	0.18	0.21	0.15	0.38	0.23	0.18
Na_2O	bdl	bdl	bdl	bdl	bdl	bdl	bdl	bdl	bdl	bdl	bdl	bdl	bdl
Total	99.92	99.74	100.1	98.51	97.83	98.19	97.74	97.16	97.36	98.18	97.54	97.69	97.59

No. Of Cations On The Basis Of 6 Oxygens

Si	1.86	1.84	1.91	1.89	1.89	1.88	1.92	1.92	1.85	1.88	1.84	1.86	1.84
Al	0.21	0.23	0.13	0.18	0.18	0.20	0.10	0.10	0.20	0.18	0.20	0.21	0.21
Ti	0.03	0.04	0.02	0.02	0.03	0.03	0.02	0.02	0.05	0.03	0.06	0.04	0.04
Fe^{2+}	0.23	0.22	0.25	0.20	0.24	0.21	0.24	0.24	0.31	0.26	0.43	0.29	0.33
Fe^{3+}	0.02	0.02	0.0	0.0	0.0	0.0	0.0	0.0	0.0	0.0	0.01	0.0	0.01
Mg	0.80	0.81	0.88	0.91	0.89	0.90	0.88	0.89	0.80	0.83	0.74	0.81	0.80
Ca	0.85	0.85	0.79	0.77	0.76	0.77	0.80	0.79	0.78	0.79	0.71	0.78	0.76
Cr	0.01	0.01	0.01	0.01	0.01	0.01	0.02	0.03	0.01	0.01	0.01	0.01	0.01
Mn	0.00	0.00	0.01	0.00	0.00	0.00	0.01	0.01	0.01	0.00	0.01	0.01	0.01
Wo	45.29	45.18	41.20	41.19	40.13	40.87	41.44	40.97	41.31	41.97	37.49	41.62	40.41
Fs	12.05	11.59	12.99	10.47	12.58	11.02	12.57	12.37	16.45	13.81	23.06	15.44	17.36
En	42.66	43.24	45.81	48.33	47.29	48.11	45.99	46.66	42.24	44.22	39.44	42.95	42.23

[1] in percent by weight

Table IIc. Amphibole Analyses[1,2]

No.	3466	4662	346A	2715	2712	66A5	36B2	6B11	1893	8932	1431	3413	3410	2737	2753	3694	3B61	32B6
SiO_2	40.99	40.36	44.37	42.06	41.91	41.57	42.10	42.13	39.55	39.13	45.77	40.42	39.72	40.90	46.74	40.49	44.87	40.82
Al_2O_3	11.24	12.16	8.34	11.24	10.65	11.14	11.15	10.64	14.05	14.47	9.54	10.82	12.00	10.46	8.41	12.12	12.44	11.12
TiO_2	4.51	4.63	3.18	4.68	5.13	4.66	4.30	4.85	4.44	4.66	3.08	5.95	5.20	3.42	2.00	4.60	3.42	4.75
FeO	17.33	15.44	19.84	16.75	16.11	15.55	16.07	15.88	15.62	16.01	15.58	16.59	14.76	17.04	15.57	11.66	14.62	18.09
MgO	10.77	11.66	10.04	16.11	10.82	12.21	11.43	11.82	10.37	10.03	9.06	10.21	11.20	11.46	10.15	13.57	8.98	8.68
CaO	9.84	10.22	9.34	10.82	10.90	10.04	10.23	10.08	10.64	10.88	10.80	10.56	10.65	10.09	11.06	11.08	9.38	10.75
MnO	0.24	0.19	0.46	10.90	0.24	0.25	0.23	0.21	0.20	0.21	0.25	0.24	0.22	0.27	0.27	0.25	0.17	0.26
Na_2O	2.40	2.54	1.45	0.24	2.18	2.56	2.26	2.14	2.74	2.56	2.49	2.42	2.68	bdl	1.19	3.70	4.70	bdl
K_2O	0.08	0.11	0.08	2.18	0.09	0.09	0.08	0.09	bdl	0.07	0.14	0.19	0.15	0.10	0.09	0.16	bdl	0.08
H_2O	2.60	2.68	2.89	0.09	1.96	1.93	2.13	2.16	2.38	1.99	3.30	2.60	3.40	6.26	4.50	2.38	1.42	5.45

No. Of Cations On The Basis Of 23 Oxygens

Si	6.19	6.06	6.73	5.64	6.26	6.19	6.28	6.28	5.93	5.86	6.84	6.12	6.02	6.36	7.04	6.01	6.56	6.33
Al	2.00	2.15	1.49	1.78	1.87	1.95	1.96	1.87	2.48	2.56	1.68	1.93	2.14	1.92	1.49	2.12	2.15	2.03
Ti	0.51	0.52	0.36	0.47	0.58	0.52	0.48	0.54	0.50	0.52	0.35	0.68	0.59	0.40	0.23	0.51	0.38	0.55
Fe^{2+}	2.19	1.94	2.52	1.88	2.01	1.94	2.00	1.98	1.96	2.01	1.95	2.10	1.87	2.22	1.96	1.45	1.79	2.35
Mg	2.42	2.61	2.27	3.22	2.41	2.71	2.54	2.62	2.32	2.24	2.02	2.30	2.53	2.66	2.28	3.00	1.96	2.01
Ca	1.59	1.64	1.52	1.55	1.74	1.60	1.63	1.61	1.71	1.75	1.73	1.71	1.73	1.68	1.78	1.76	1.47	1.79
Mn	0.03	0.02	0.06	1.24	0.03	0.03	0.03	0.03	0.03	0.03	0.03	0.03	0.03	0.04	0.03	0.03	0.02	0.03
Na	0.70	0.74	0.43	0.06	0.63	0.74	0.65	0.62	0.80	0.74	0.72	0.71	0.79	0.0	0.35	1.06	1.33	0.0
K	0.02	0.02	0.02	0.37	0.02	0.02	0.02	0.02	0.0	0.01	0.03	0.04	0.03	0.02	0.02	0.03	0.0	0.02

[1] in percent by weight
[2] the total of all oxides including water is 100%
bdl below detection limit

IX. Appendix III: Construction of fO_2 - pH Diagrams

The principles of consrtuction of the fO_2 – pH diagrams are given in detail by Barnes and Kullerud (1961) and will be only briefly reviewed here.

The equilibrium constant, K, of a reaction is given as:

K = activity product of products / activity product of reactants

and the *log* K can be expressed as:

$$\log K = \sum \log a_i - \sum \log a_j$$

where i is the number of product species and j is the number of reactant species. When oxygen or hydrogen ion is a component species of a reaction, its activity can be calculated from the above relationship if the activities of all other species are known.

The equillibrium constant of a reaction is related to the free energy change in the reaction, ΔG_r, as follows:

$$-\log K = \Delta G_r / 2.303\, RT$$

where, R is the gas constant and T is the temperature in K. The free energy change in the reaction can be calculated as:

$$\Delta G = \sum \Delta G_{i,f}^{P,T} - \sum \Delta G_{j,f}^{P,T}$$

where ΔG and ΔG are the standard molal free energies of formation of the ith and jth, reactant and product species.

For minerals and gases,

$$\Delta G_i^{P,T} = \Delta G_{i,f}^{\circ} - S^{\circ}(T - Tr) + \int_{Tr}^{T} C_p^{\circ}\, dT - T \int_{Tr}^{T} C_p^{\circ}\, d\, lnT + V^{\circ} dP$$

(Helgeson *et al.*, 1978)

where,

Pr, Tr = Pressure and temperature of reference, i.e. 1 bar and 298.15 K.

$\Delta G_{i,f}^{\circ}$ = Standard Gibbs free energy of formation of the ith species in its standard state.

$\Delta G_i^{P,T}$ = Standard molal Gibbs free energy of the ith species at specified temperature and pressure.

S°, V°, C_p° = standard molal entropy, volume and heat capacity of the ith species.

The apparent standard molal Gibbs free energy for an aqueous species, at given temperature and pressure, can be calculated as:

$$G^{P,T}_{j,f} = G^{\circ}_{f,j} - S^{\circ}_{j}(T-T_r)$$
$$-C_{1,j}(T\ln(T/T_r) - T + T_r)$$
$$+ C_{2,j}(T - T_r - (T - \Theta_j)\ln(T-\Theta_j / T - \Theta_j)$$
$$+(2(a_{1,j}(T - \Theta) + a_2 T)(P - P_r) + a_{3,j}(T - \Theta_j) + a_4 T (P^2 - P_r^2)) / 2 (T-\Theta_j)$$
$$W_j (Z_{P,T} - Z_{P_r,T_r} - Y (T - T_r))$$

Helgeson *et al.* (1981)

where, $G^{\circ}_{f,j}$ = apparent standard Gibbs free energy of formation of jth species.

S°_j = standard molal entropy of the jth species.

C_{1j}, C_{2j} = heat capacities of the jth species.

$a_{1j}, a_{2j}, a_{3j}, a_{4j}$ = temperature and pressure independent coefficents for the jth species.

$Z = -1 / \epsilon^{\circ}$

W_j = born coefficient for the jth species.

Y = negative derivative of the dielectric constant of water at T and P.

T_r, P_r = temperature and pressure of reference.

T,P = temperature and pressure of interest.

The standard states of the mineral, gases and aqueous species were seperately defined. The Standard state for a mineral is its pure form with a unit activity, at T and P; and that for a gas is an ideal gas with unit fugacity at T and 1 bar. The standard state of an aqueous species is a hypothetical 1 molal solution at T and 1 bar.

Table IIIa. Reactions and Equilibrium Constants Used in Constructing Figures 14 and 15

Reaction	Log K 250°C	Log K 300°C
$H_2S = H^+ + HS^-$	-7.35	-8.06
$H_2S + 2\ O_2 = H^+ + HSO_4^-$	61.90	53.30
$H_2S + 2\ O_2 = 2\ H^+ + SO_4^{=}$	56.49	47.24
$HS^- + 2\ O_2 = SO_4^{=} + H^+$	63.84	55.30
$HSO_4^- = SO_4^{=} + H^+$	-5.41	-6.06
$Fe^{2+} + Cl^- = FeCl^+$	2.34	2.33
$Cu^+ + Cl^- = CuCl^0$	2.30	2.80
$FeS + 2\ H^+ + Cl^- = FeCl^+ + H_2S$	2.56	4.40
$FeS_2 + 2\ H^+ + Cl^- + H_2O = FeCl^+ + 2\ H_2S + {}^1/_2\ O_2$	-19.47	-14.64
$Fe_3O_4 + 6\ H^+ + 3\ Cl^- = 3\ FeCl^+ + 3\ H_2O + {}^1/_2\ O_2$	-2.43	3.76
$CuFeS_2 + H^+ + {}^1/_4\ O_2 + Cl^- = FeS_2 + {}^1/_2\ H_2O + CuCl$	9.70	9.80
$3\ FeS_2 + 11\ O_2 + 6\ H_2O = Fe_3O_4 + 6\ SO_4^{=} + 12\ H^+$	281.40	234.60
$3\ FeS_2 + 6\ H_2O = Fe_3O_4 + 6\ HS^- + 6\ H^+ + O_2$	-101.71	-97.32
$2\ FeS_2 + 7.5\ O_2 + 4\ H_2O = Fe_2O_3 + 4\ HSO_4^- + 4\ H^+$	215.12	185.81

$2\ FeS_2 + 7.5\ O_2 + 4\ H_2O = Fe_2O_3 + 4\ SO_4^{=} + 8\ H^+$	193.48	161.57
$2\ Fe_3O_4 + {}^1/_2\ O_2 = 3\ Fe_2O_3$	17.65	15.51
$3\ FeS + 3\ H_2O + {}^1/_2\ O_2 = Fe_3O_4 + 3\ H_2S$	10.19	9.93
$3\ FeS + 3\ H_2O + {}^1/_2\ O_2 = Fe_3O_4 + 3\ HS^- + 3\ H^+$	−11.86	−14.25
$FeS + H_2S + {}^1/_2\ O_2 = FeS_2 + H_2O$	22.60	19.63
$3\ FeS_2 + 6\ H_2O + 11\ O_2 = Fe_3O_4 + 6\ HSO_4^- + 3\ H^+$	313.86	270.96
$3\ FeS_2 + 6\ H_2O = Fe_3O_4 + 6\ H_2S + O_2$	−57.57	−48.86
$Mg_3Si_4O_8\ (OH)_2 + 6\ H^+ = 3\ Mg^{++} + 4\ SiO_2 + 4\ H_2O$	8.45	6.24
$4\ FeS_2 + Cu_5FeS_4 + 2\ H_2O = 5\ CuFeS_2 + 2\ H_2S + O_2$	−39.57	−34.12